

INVESTIGATION OF IMPROVED HANDOVER
APPLYING MIMO SYSTEMS AND INTELLIGENT
CONTROL TECHNOLOGIES FOR MOBILE
COMMUNICATIONS

By

JIN-BAEK KIM

Bachelor of Engineering

Kangwon National University

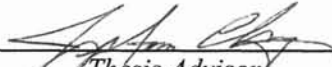
Chunchon, Korea

2000

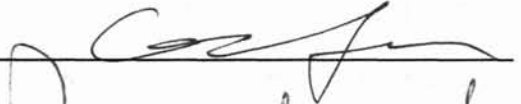
Submitted to the Faculty of the
Graduate College of the
Oklahoma State University
in partial fulfillment of
the requirements for
the Degree of
MASTER OF SCIENCE
December, 2002

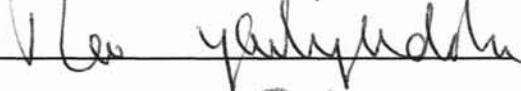
INVESTIGATION OF IMPROVED HANDOVER
APPLYING MIMO SYSTEMS AND INTELLIGENT
CONTROL TECHNOLOGIES FOR MOBILE
COMMUNICATIONS

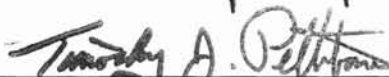
Thesis Approved:



Thesis Advisor







Dean of the Graduate College

PREFACE

One of the fundamental objectives of mobile communications is to afford untethered seamless communications. Handover plays an important role in providing seamless communications. However, the emerging wireless communication networks consist of conventional voice traffic and data traffic, as well. Thus, the characteristics of emerging traffic types are no longer homogeneous, they are heterogeneous. Compared to conventional homogeneous voice communication network, where voice quality is a major concern of QoS, the heterogeneous integrate communication network requires different QoS provisions, such as minimizing the bit error rate (BER), and/or maximizing the link capacity, etc. Therefore, the handover procedure in emerging broadband integrated services communication networks would be improved by introducing multivariable decision parameters for maintaining the different QoS requirements.

Meanwhile, the importance of efficient spectrum utilization cannot be overemphasized in wireless mobile communication systems, where available frequency spectrum is extremely scarce. Recent advance in information theory has revealed unprecedented improvements on spectral efficiency by employing multiple antennas both at the transmitter and the receiver sites. Although many research efforts have been devoted to analyze the spectral efficiency of this dual array antenna system, the analysis of handover control and QoS support for the dual array antenna systems has not been conducted yet, and therefore it is the focus of this thesis.

ACKNOWLEDGMENTS

I wish to express my deep and sincere thanks and gratitude to my advisor Dr. Jong-Moon Chung for his supervision, support, critical suggestions, and inspiration without whom this thesis would not have been possible. My appreciation and thanks are also due to my committee members Dr. R. K. Yarlagadda and Dr. Guoliang Fan for their invaluable support, assistance, encouragement and guidance throughout my Master's program here at the Oklahoma State University.

I would like to thank the Advanced Communication Systems Engineering Laboratories (ACSEL) and the Oklahoma Communication Laboratory for Networking and Bioengineering (OCLNB) of the Oklahoma State University for supporting resources. I would like to thank my group members for their contribution. I would also like to thank other members of the ACSEL laboratories for their recommendations and support and my friends who made my thesis work an enjoyable and pleasant one. In addition, I sincerely appreciate Dr. Wun-Cheol Jeong for his special guidance, my parents and my friends for their support and encouragement throughout my masters program.

TABLE OF CONTENTS

Chapter	Page
I. INTRODUCTION.....	1
1.1 Motivation.....	1
1.2 Objective.....	2
1.3 Overview.....	2
II. BACKGROUND RESEARCH.....	3
2.1 The history of mobile and personal communications.....	3
2.1.1 The first generation mobile communication systems.....	4
2.1.2 The second generation mobile communication systems..	4
2.1.3 Analog cellular systems.....	5
2.1.3.1 AMPS.....	5
2.1.3.2 TACS.....	6
2.1.3.3 NMT.....	6
2.1.3.4 NTT.....	6
2.1.4 Digital cellular systems.....	7
2.1.4.1 GSM.....	7
2.1.4.2 IS-136.....	11
2.1.4.3 PDC.....	13
2.1.4.4 IS-95.....	13
2.1.4.5 PCS in North America.....	15
2.1.4.6 IMT-2000 standards.....	15
2.2 Handover operations in mobile communication systems.....	17
2.2.1 Handover operation for the 1 st generation systems.....	17
2.2.2 Handover for the 2 nd generation systems.....	18
2.2.3 MAHO	20
2.2.4 Handover parameters.....	21
2.2.5 Generalization of Handover.....	21
2.2.6 Types of Handover.....	22
2.2.7 Handover scenario and conventional method.....	24
2.2.8 Received signal strength.....	25
2.2.9 Received signal strength with hysteresis.....	25
2.2.10 Received signal strength with hysteresis and threshold...25	

Chapter	Page
2.3	Dual array antenna system..... 26
2.3.1	Information channel capacity of conventional system....26
2.3.2	Information channel capacity of DAA system..... 27
2.3.3.1	Steered Directive array..... 29
2.3.3.2	Transmit Diversity.....31
2.3.3.3	Dual array antenna system..... 33
III.	INTELLIGENT HANDOVER CONTROL TECHNOLOGIES.....35
3.1	Handover Management.....35
3.1.1	Problem description..... 37
3.1.2	Fuzzy logic method37
3.1.3	Fuzzy logic solution.....38
3.2	Pattern recognition by Artificial Neural Network (ANN)..... 44
3.2.1	Basic property of LVQ..... 44
3.2.2	Using LVQ for pattern recognition.....46
3.2.3	LVQ learning algorithm..... 47
3.3	Inter-system handover procedure for IMT-2000..... 51
3.3.1	Handover into a boundary cell.....51
3.3.2	Handover into a new system..... 52
3.3.3	Performance evaluation..... 53
3.3.4	Probability of ISHO.....54
3.3.5	Boundary cell area..... 58
IV.	MIMO SYSTEMS BASED HANDOVER TECHNOLOGIES..... 61
4.1	Introduction.....61
4.2	Steered directive array system..... 63
4.3	Transmit diversity.....67
4.4	DAA diversity.....70

Chapter	Page
V. CONCLUSIONS.....	73
VI. REFERENCES.....	75
VII. APPENDIX A.....	80
APPENDIX B.....	81

LIST OF FIGURES

Figure	Page
2.1 Speech encoding and modulation in GSM.....	10
2.2 Handover Operation.....	18
2.3 Mobility management operations.....	19
2.4 Soft Handover.....	23
2.5 Hard Handover.....	23
2.6 Signal strength vs. Distance when user is moving from cell A to cell B.....	24
2.7 Illustration of Steered Directive array.....	29
2.8 Single user data rate supported in 90 % of locations vs. range	30
2.9 Illustration of Transmit Directive array.....	31
2.10 Single user data rate supported in 90 % of locations vs. range.....	32
2.11 Multiple receiver – multiple transmitter.....	33
2.12 Single user data rate supported in 90 % of locations vs. range for DAA.....	34
3.1 Block diagram of Fuzzy logic-ANN handover algorithm.....	36
3.2 RSS.....	39
3.3 MS – BS distance.....	40
3.4 Fuzzy sets of handover factor.....	41
3.5 Result of the min-max solution.....	43
3.6 HO factor.....	43
3.7 Block Diagram of LVQ.....	45

Figure	Page
3.8	Approximated division for grouping..... 46
3.9	Changed version of Figure 3.8..... 47
3.10	Classified groups.....48
3.11	Signal flow for Handover into a boundary cell..... 51
3.12	Signal flow for Handover into the next system..... 52
3.13	Probability of ISHO for Indoor network.....58
3.14	Probability of ISHO for Pedestrian network..... 59
3.15	Probability of ISHO for vehicular network..... 59
3.16	Probability of ISHO for high speed network..... 60
4.1	Soft handover situation when user is moving from cell A to cell B..... 62
4.2	Capacity outage vs. distance for phase steered directive array..... 64
4.3	Single user data rate vs. distance with M-steered directive array..... 65
4.4	Probability of capacity vs. capacity threshold with steered directive array.. 66
4.5	Capacity outage vs. distance with M antenna transmit diversity.....68
4.6	Probability of capacity vs. capacity threshold with transmit diversity..... 69
4.7	Capacity outage vs. distance with DAA diversity.....70
4.8	Probability of capacity vs. capacity threshold with DAA diversity.....71

LIST OF TABLES

Table	Page
1. System Parameters of GSM.....	9
2. System Parameters of IS-136.....	12
3. Comparison of the second and the third generation systems.....	16
4. Rule of Fuzzy sets.....	42
5. System Parameters.....	56
6. Additional Signaling Time Required for Performing ISHO for IMT-2000...	57
7. A comparison of the capacity gain for the three topologies.....	72

CHAPTER I

Introduction

1.1 Motivation

One of the fundamental objectives of mobile communications is to provide high quality broadband untethered seamless communications to the mobile users. Handover plays an important role in providing seamless communications. Conventionally, mobile communication networks carry homogeneous traffic, e.g., voice packets, where identical quality of service (QoS) provision is required. In such communication networks, a single parameter, such as the signal strength, may provide sufficient information to determine when to initiate and perform the handover operation.

However, the emerging wireless communication networks consist of voice traffic and data traffic. Thus, the characteristics of emerging traffic types are no longer homogeneous, but are rather heterogeneous. Compared to conventional homogeneous voice communication networks, where voice quality was the only major concern, the voice and data combined heterogeneous integrated traffic requires different communication network QoS provisions, such as minimizing bit error rate (BER), and/or maximizing link capacity, etc. Therefore, the handover procedures in emerging broadband integrated services communication networks would be improved by introducing multivariable decision parameters for maintaining the different QoS requirements.

Meanwhile, the importance of efficient spectrum utilization cannot be overemphasized in wireless mobile communication systems, where the available frequency is extremely scarce. Recent advance in information theory has revealed unprecedented improvements on spectral efficiency by employing multiple antennas both at the transmitter and at the receiver sites. Although many research efforts have been devoted to analyze the spectral efficiency of this dual array antenna system, the analysis of handover for the dual array antenna systems have not been conducted yet.

1.2 Objective

In this thesis, we mainly focus on two fundamental problems related to handover. First, we propose and analyze a fuzzy logic and artificial neural network algorithm for multivariable optimization in handover decision procedures. Fuzzy logic and artificial neural network based handover algorithms are predicted to perform better than hard decision based algorithms, especially when multivariable optimization techniques are applied. In our analysis, the Fuzzy logic and artificial neural network algorithm is adopted for the handover initiation and decision procedures.

Also, we analyze the attainable capacity during handover procedures for various system configurations. In broadband communications, a certain data rate should be sustained to meet the QoS requirements even during handover procedures. We compare capacity outage probabilities between conventional cellular systems and dual array antenna systems that have gained much attention recently.

1.3 Overview

The rest of the thesis is organized as follows. In chapter 2, background information on handover technology is explained and overviewed. First, historic mobile communication systems and handover technologies are overviewed. And then multi-input multi-output (MIMO) wireless technology is addressed. In Chapter 3, intelligent handover management techniques of the third generation wireless systems are introduced. In Chapter 4, the capacity outage performance is analyzed for various types of system configurations. Finally, we conclude our investigation and provide a brief summary of this thesis in Chapter 5.

CHAPTER II

Background Research

The purpose of this chapter is to provide a common framework to help understand the topics related to the main scope of this thesis. Section 2.1 provides an overview of mobile and personal communication systems from the first generation wireless communication networks to the third generation wireless communication networks. Section 2.2 provides an introduction of handover technologies in mobile communication systems. In addition, section 2.3 is devoted to the introduction of dual array antenna systems employing multiple antennas both at the transmitter and the receiver sites.

2.1 The history of mobile and personal communications

Radio communications can trace their origins to the discovery of electromagnetic waves by Hertz in 1888 and the subsequent demonstration of transatlantic radio telegraphy by Marconi in 1901 [4]. Mobile radio systems use simplex channels. Originally simplex channels were introduced for police and emergency services. In the 1970s, the concept of cellular was in a defining stage, which played a major role in the development of mobile communication systems and networks around the world. Implementation of analog and digital systems represents a change for the designing capabilities of mobile communication systems. The requirements of future mobile communication systems can be summarized as follows [4]:

- enlarged capacity and coverage areas
- world wide service coverage using global satellite and mobile communications services
- interoperability between heterogeneous radio technologies
- enhanced reliability even under high speed roaming conditions

2.1.1 The first generation mobile communication systems

From the beginning of the public mobile radio systems in the United States in 1946 until the first analog cellular system went into operation in Chicago, mobile systems were mainly based upon the trunking principle [2]. The available frequency spectrum was divided into a suitable number of frequency channels. A high power, centralized antenna was installed to transmit signals to mobile receivers. Large mobile receivers were also installed in vehicles, and telephone sets were also big. Since a call from a mobile terminal had to compete among call-requests from other users to obtain a channel from the limited number of channels, the probability of call blocking was very high in first generation mobile communication systems. The performance of these systems was also limited in terms of their coverage area and capacity. In the automated mobile telephone system (AMTS), after mobile user presses the send button, the receiver starts scanning for an idle channel by cycling through all the channels in the system. Although these systems provided an improvement in the quality of service, they still possessed some interesting performance modeling problems [1].

2.1.2 The second generation mobile communication systems

Since the initial commercial introduction of the advanced mobile phone system (AMPS) service in 1983, mobile communications has grown tremendously [2]. Besides the frequency reusing capabilities provided by the cellular operations, advanced technologies for wireless communications, digital signal processing, and the increased battery capabilities have contributed to the tremendous growth of mobile communications. While the first generation mobile communication systems were characterized as analog cellular systems, the digital cellular, low power wireless, and personal communication systems (PCS) are categorized as the second generation mobile communication systems [2]. In the United States, the implementation of digital cellular standards was developed by the Telecommunications Industry Association (TIA). These standards are mainly based upon time division multiple access (TDMA) and code division multiple access (CDMA) technologies. The systems are originally designed to operate with dual mode systems such that they support backward compatibility with the first generation mobile communication systems, such as AMPS systems. Meanwhile, a third digital cellular

system referred to as the personal digital cellular was developed in Japan, and the specifications for these second generation cellular systems are being developed to satisfy the various business applications and mandatory legal requirements of specific countries. International Mobile Telecommunications 2000 (IMT-2000) is the standard under development by the International Telecommunication Union (ITU) to set the stage for the third generation of mobile communication systems. The IMT-2000 standard is expected to ensure global mobility and consolidate different wireless environments into a single standard [3].

2.1.3 Analog Cellular Systems

2.1.3.1 Advanced Mobile Phone System

Advanced mobile phone system (AMPS) was developed by Bell Laboratories and the first AMPS service was tested and implemented in Chicago [4]. Cellular mobile service licenses for an initial 40 MHz spectrum in the 800 MHz frequency band were issued, and finally an additional 10 MHz was added. Therefore, the spectrum allocation for current AMPS mobile radio frequency band in the United States is 50 MHz within 824-849 MHz for uplink and 869-894 MHz for downlink. AMPS standard allocates carriers spaced 30 kHz for this 50 MHz spectrum, thereby, there are total of 832 full duplex channels with 416 channels each for the A-band and the B-band operations in each licensing area. Out of 416 channels, 21 channels are used as control channels and the remaining 395 channels are used for user traffic. Each channel carries data at 10 kbps with Manchester coding, where the bit rate can be extended up to 20 kbps [4]. Frequency shift keying (FSK) is employed as the modulation scheme, and Bose-Chaudhary encoding is used to combat the multipath fading errors. For the speech or voice channel, a blank and burst technique is used, whereby the voice signal is blanked approximately 50 ms and a data burst of 10 kbps is inserted into the voice channel [4]. This signaling is used to alert the mobile station that the channel-transfer is about to be taken over for an impending handover. In cellular systems, a frequency band employed at a reference cell is reused at a distant cell located far apart. Since the same frequency is reused spatially, the capacity of the whole cellular network is increased. However, interfering signals will steadily come from the co-channel cells. To reduce this adverse effect of co-channel

interference, AMPS technology divides the total available frequency band into 12 group frequency clusters with omnidirectional antennas at the base station site, or into 7 group cluster with three 120 degree sectors per cell.

2.1.3.2 Total Access Communication System

Total Access Communication System (TACS) developed in the United Kingdom is an adaptation of AMPS to suit European frequency allocations [4]. It uses a 50 MHz spectrum in the 890-915 MHz range for uplinks and the 935-960 MHz range for downlinks. The 25 kHz channel spacing is specified and the TACS provides 1000 full duplex channels. The speech frequency deviation is ± 9.5 kHz in peak and the data transmission frequency deviation is ± 6.4 kHz at a 8 kbps rate. Only the first 600 channels were assigned to the two analog mobile network operators in the United Kingdom.

2.1.3.3 The Nordic Mobile Telephone System

The Nordic Mobile Telephone (NMT) was implemented in Denmark, Norway, Sweden, and Finland, using the 450 MHz band, named NMT-450. Later, NMT-450 was upgraded to NMT-900 to occupy 50 MHz in the 890-915 MHz and 935-960 MHz band [4]. The NMT-450 was designed to provide full roaming capability within the Nordic countries. The signaling rate of this system is 1.2 kbps employing fast frequency shift keying (FFSK) scheme with convolution forward error correcting code.

2.1.3.4 The Nippon Telegraph and Telephone System

The first Nippon Telegraph and Telephone (NTT) system in the 800 MHz band was introduced in Japan with a 30 kHz allocation in the 925-940 MHz for uplink and 870-885 MHz for downlink bands with 25 kHz channel spacing and a control channel signaling rate of 300 bps [4]. The frequency allocation provides for 56 MHz in the 860-885/915-940 MHz and 843-846/898-901 MHz frequency bands with channel spacing of 25 kHz. The high capacity system uses a reduced channel spacing of 12.5 kHz and an increased control channel signaling rate of 2400 bps.

2.1.4 Digital Cellular Systems

Compare to analog cellular systems, digital cellular systems have many advantages which are summarized below [4]:

- capacity increase over analog systems
- reduced transmission power and longer battery life
- wide area roaming capability
- better security (terminal validation and user identification)
- compatibility with ISDN, leading to a wider range of digital service
- ability to operate in small cell environments

2.1.4.1 GSM : The European TDMA Digital Cellular standard

The characteristics of the initial GSM standard include [5]:

- fully digital system utilizing the 900 MHz frequency bands
- TDMA over radio carriers
- 8 full-rate or 16 half rate TDMA channels per carrier
- user/terminal authentication for fraud control
- encryption of speech and data transmission over the radio path
- full international roaming capability
- low speed data rate (maximum 9.6 kbps)
- compatibility with ISDN for supplementary services
- supporting of short message services

The reference architecture and associated signaling interfaces for GSM are aligned with those specified in ITU-T Recommendation Q.1001 [5]. The GSM mobile stations are portable units that can be used on any GSM system as a moving unit. Power levels supported by the GSM mobile station range from 0.8 to 8.0 W, and power saving techniques are used on the air interface to extend battery life. A subscriber identity module (SIM) is required to activate and operate a GSM terminal. The base station system comprises a base station controller (BSC) and one or more subtending base

transceiver station (BTS). The base station switch (BSS) is responsible for all functions related to the radio resource management, such as [5]:

- Radio resource control
- Frequency hopping and power control
- Handover management
- Digital signal processing

The mobile switching center for GSM can be viewed as a local ISDN switch with additional capabilities to support mobility management functions, i.e. [5]:

- Call setup, supervision, and release
- Digit collection and translation
- Call routing
- Mobility management
- Paging and alerting
- Radio resources management during a call
- Echo elimination

The Home Location Register (HLR) represents a centralized database that has the permanent datafill about the mobile subscribers in a large service area. Usually one HLR is deployed for each GSM network for administration of subscriber configuration and service. HLR maintains the following subscriber's data on a permanent basis [5]:

- international mobile subscriber identity
- service subscription information
- service restrictions
- supplementary services
- mobile terminal characteristics
- billing information

The Visiting Location Register (VLR) represents a temporary data store, and generally there is one VLR per MSC. This information contains which subscriber is currently in the service area covered by the MSC/VLR. The VLR includes these information [5]:

- features currently activated
- temporary mobile station identity

- current location information about the MS

The GSM uses time division multiple access (TDMA) and frequency division multiple access (FDMA), whereby the available 25 MHz spectrum is divided into 124 carriers, and each carrier is divided into 8 time slots. Therefore, several conversation can take place over the same pair of transmit / receive radio frequencies [5].

System Parameters	Value (GSM)
Multiple access	TDMA/FDMA/FDD
Uplink frequency	890-915 MHz
Downlink frequency	935-960 MHz
Channel bandwidth	200 kHz
Number of channels	124
Channels/carrier	8 (full rate), 16 (half rate)
Frame duration	4.6 ms
Interleaving duration	40 ms
Modulation	GMSK
Speech coding method	RPE-LTE convolution
Speech coder bit rate	13 kbps (full rate)
Associated control channel	Extra frame
Handover scheme	Mobile-assisted
Mobile station power levels	0.8, 2, 5, 8 W

Table 1. System Parameters of GSM.

In the GSM system, digitized speech can be passed at 64 kbps through a transcoder, which compresses the 64 kbps PCM speech to a 13 kbps data rate [5].

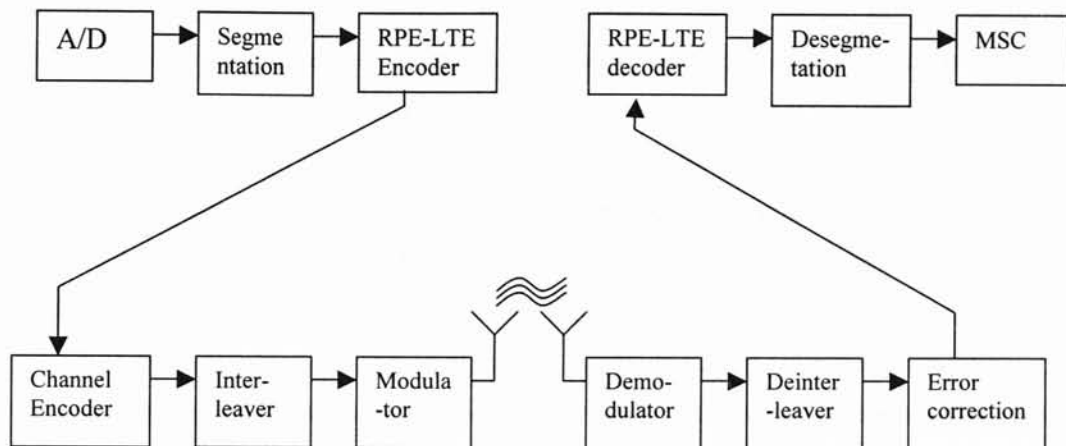


Figure 2-1. Speech encoding and modulation in GSM.

The speech coding technique improves the spectral efficiency of the radio interface. The GSM transcoder also allows the detection of silent interval in the speech sample, during which transmit power at the mobile station can be turned off in order to save power and extend battery life. The transcoded speech is error detected by passing it through a channel encoder, which utilizes not only a parity code, but also a convolution code. The channel encoding bit rate of transcoded speech can go up from 13 kbps to 22.8 kbps for the GSM full rate coder. A half rate GSM coder has also been specified. The 456 bits of the encoded data uses convolutional coding techniques. An interleaving depth of 8 is used in GSM full rate speech. There are two separable categories of logical channels in GSM: traffic channels (TCH) and control channel (CCH). There are three types of control channels: broadcast (BCCH), common (CCCH), and dedicated (DDCH), each of which is further subdivided. The broadcast control channel is a unidirectional channel that is used to broadcast information regarding the mobile serving cell and neighboring cells. A common control channel may be used either for uplink or downlink communications. The paging and access grant channels operate in the downlink direction. The dedicated

control channel is used for call set up, or for measurement and handover, and is assigned to a single mobile connection. To alleviate the effect of multipath fading when a mobile station is stationary or moving slowly, GSM provides a frequency-hopping capability on the radio interface. GSM utilizes voice activated transmissions or discontinuous transmission to maximize the spectrum efficiency. This technique is based on detecting voice activity and switching on the transmitter only during periods when there is active speech to transmit. The GSM signaling at the radio interface consists of LAPDm at layer 2. LAPDm is a modified version of LAPD. Layer 3 is divided into three sublayers that deal with radio resource management (RM), Mobility management (MM), and connection management (CM). The RR is concerned with managing logical channels, including the assignment of paging channels, signal quality measurement reporting, and handover. The MM provides functions necessary to support user/terminal mobility, such as terminal registration, terminal location updating, authentication, and IMSI detach/attach. The CM is concerned with call and connection control, establishing and clearing connections, management of supplementary services, and support of the short message service [5].

2.1.4.2 IS-136: The North American TDMA Digital cellular standard

IS-136 supports a wide range of basic and supplementary services. IS-136 standard includes the following [6]:

- short message service (SMS) – point to point
- emergency service.
- lawfully authorized electronic surveillance.
- on the air activation
- sleep mode terminal operation
- rolling mask message encryption

Further, IS-136 will provide a complete range of supplementary service categories, and these include [6]:

- Call Forwarding services
- Call termination services

- Call origination services
- Multiple-party services
- Call restriction services
- Privacy services

System Parameters	Value(GSM)
Multiple access	TDMA/FDD
Uplink frequency	824-849 MHz
Downlink frequency	869-894 MHz
Channel bandwidth	30 kHz
Number of channels	832
Channels/carrier	6
Frame duration	40 ms
Interleaving duration	27 ms
Modulation	$\pi/4$ QPSK
Speech coding method	VSELP convolution
Speech coder bit rate	13.2 kbps (full rate)
Associated control channel	Same frame
Handover scheme	Mobile-assisted
Mobile station power levels	0.8, 1, 2, 3 W

Table 2. System Parameters of IS-136 [6].

The network reference model is the same for both the TDMA-based and CDMA based radio systems. The reference architecture and interface reference points are almost same as those for GSM. Nevertheless these similarities in the reference architecture and interface reference points, the protocols and messages deployed in the IS-136 for intersystem operation are quite different from those of the GSM. IS-136 will utilize the currently allocated spectrum for analog AMPS [6]. Each frequency channel is time

multiplexed with a frame duration of 40 ms, which is separated into six time slots of 6.67 ms duration. For mobile to base communication in an IS-136 system using a full rate codec, three mobiles transmit to a single base station radio by sharing some frequency. In order to achieve this, each mobile station transmits periodic bursts of information to the base station in a predetermined order.

2.1.4.3 PDC: The Japanese TDMA Digital Cellular Standard

In April 1991 the Research and Development Center for Radio Systems of Japan finished the detailed standard for the Japanese digital cellular system, now known as PDC (Personal Digital Cellular). The PDC radio interface has outstanding features that the system designers believe are superior to the GSM system. These features are following [6]:

- PDC adapts diversity reception in the mobile stations which obviates the need for equalizers, which are an essential component of GSM.
- PDC uses a lower transmission bit rate (43 kbps vs. 270.83 kbps), which leads to better spectrum utilization, higher capacity, and lower cost.
- The access signaling protocols in the PDC are simpler and require fewer procedures.

The signaling structure for the PDC was developed to ensure efficient spectrum utilization, support of enhanced services, and alignment with the open system interconnection model, and the ITU signaling recommendations. The PDC standard essentially specifies the radio interface and leaves the individual operators to decide the network configuration they wish to implement. The network configuration provides connectivity to fixed networks, ensures roaming between different PDC cellular networks, and uses a unified interface for interconnection of the PDC cellular network to the fixed network.

2.1.4.4 IS-95: The North American CDMA Digital Cellular Standard

Some of the features and services that have been standardized as part of the IS-95A standard include the following [7]:

- Short Message Service will support both mobile terminated and mobile originated short messages of up to 255 octets on either the control channel or traffic channel.
- Slotted paging enables mobiles to wake up for one to two times slots per slotted paging cycle to listen to incoming pages
- Over the air activation allows the mobile to be activated by the service provider without third party intervention. It also provides potential for future remote reprogramming of mobile terminals and for software downloadable capabilities
- Enhanced mobile station provides the use of international mobile station identities based on the ITU-T standard thereby facilitating international roaming and separation of mobile DNs and mobile terminal identities
- Temporary mobile station identities allows for the allocation of TMSI by serving VLRs, which are used on the air interface to maintain user confidentiality and to reduce overall signaling traffic loads across the radio interface
- Asynchronous data and group 3 Fax
- Synchronous data applications for secure telephone unit
- Packetized data
- Supplementary services call waiting, call forwarding, and calling line ID

One of the most significant features of IS-95 CDMA systems is diversity. The types of diversity that are available in a CDMA system include the following:

- Time diversity provided by symbol interleaving, error detection, and correction coding
- Frequency diversity, provided by the 1.25 MHz wideband signal
- Space diversity, provided by the dual cell site receiving antennas, multipath rake receivers, and multiple cell sites

In a CDMA system, the mobile to base station link is subject to the near-far-problem, which considers a mobile station which is close to the base station has much lower path loss than a mobile that is far removed from the base [7]. If all the mobile stations were to use the same transmission power, the mobile which is close to the base station would effectively jam the signals from the mobiles far away from the base station. Therefore, for the CDMA system to work effectively, RF power in the system needs to be

controlled. The key parameters that determine the capacity of a CDMA digital cellular system are as follows [7]:

- Processing gain
- Energy per bit to noise power ratio
- Voice activity factor
- Frequency reuse efficiency
- number of sectors in the cell site antenna

2.1.4.5 PCS in North America

Allocation of frequency spectrum in the 2 GHz band by the FCC spurred the standardization activity on personal communication service (PCS) in North America in the early 1990s [7]. The scope of PCS covers high mobility and various applications like GSM. The frequency spectrum identified by the FCC for PCS licensed and unlicensed operation is in the 1850-1990 MHz band. In the licensed band, it provides a total of 60 MHz each for uplink and downlink transmission in the frequency division multiplex with 80 MHz separation, and a total of 20 MHz for system operating in the unlicensed band subject to the FCC specified spectrum rules. The PCS radio interface standards based on these technologies (GSM, IS-136, IS-95, WACS/PHS, and DECT) tried to maintain maximum commonality with the existing implementations, and main differences from the base standards were in the lower layers, to allow efficient operation in the 1900 MHz PCS band [7].

2.1.4.6 IMT-2000 Standards

International Mobile Telecommunications-2000 (IMT-2000) [8] has extended greatly for its service capabilities and coverage area of operating environments. One of the most important requirements for IMT-2000 is flexibility. Flexibility is necessary for supporting different environments with minimum changes in the systems. Some of the performances of IMT-2000 are [9]:

- Optimized radio channel management
- Availability of bandwidth on demand
- Dynamic channel coding

- Optimized technique for modulation and spreading
- Optimized traffic multiplexing and compression
- Smart antennas
- Increased software control of radio characteristics

Aspects	2 nd generation systems	3 rd generation systems (IMT-2000)
Digital technology	All use digital technologies for modulation, speech, channel coding, and implementation of control and data channels.	Increased use of digital technologies including programmable radios.
Commonality for different operating environments	Optimized for specific operating environments, such as, the vehicular and pedestrian environments.	A major objective is maximizing optimization of radio interfaces for multiple operating environments.
Frequency bands	Operate in multiple frequency bands, e.g., 800 MHz, 900 MHz, and 1.5 and 1.8 GHz.	Common global frequency band for both terrestrial and satellite components
Data services	Limited less than 32 kb/s	Higher transmission speed capabilities encompassing circuit and packet switched and multimedia services.
Roaming	Limited to the specific area.	Global roaming.

Table 3. Comparison of the second and the third generation mobile communication systems [9].

- Radio Aspects

Two major issues for any radio systems are the capacity and coverage area. For mobile systems which are operating in an urban area, capacity is the major requirement, while for the rural area, coverage is more important [9]. Although terrestrial based systems provide high capacity, there are limits to the coverage area. A base station can only cover a small fraction of the world's area. Satellite based systems provide

tremendous global services to mobile users in all places and all the times. In view of the geometry, the cell size is huge for satellite based systems.

- Network Aspects.

IMT-2000 radio transmission and signaling systems have to be very flexible to efficiently handle a global range of services [10]. IMT-2000 also provides fixed wireless access (FWA) capability with potential applications to developing countries for introducing basic telecommunication services in a cost effective manner [11]. The goal of the IMT-2000 is to provide identical services offered by the fixed wire line networks.

2.2 Handover operations in mobile communication systems

In cellular mobile communication systems, a subscriber migrates among cells. To support seamless communications wherever a subscriber is located, a communication link must maintain its QoS. The process of transferring a call in progress from one cell to another cell without interruption of the call is referred to as handover. Handover operation involves a mobile switching center (MSC) interworking with more than two base stations. In this section, we review handover schemes [7].

2.2.1 Handover operation for the first generation systems

Handover operations are illustrated in Figure 2-2. Base station 1 is handling the call for the mobile station (event 1). It notices the mobile station's transmission is decreasing in power (event 2). It sends a handover measurement request message to its MSC (event 3). The MSC can request a number of base stations to announce their reception of the mobile station's signal. In this example, it requests that base station 2 monitor and report back its result (events 4, 5, and 6). The MSC decides that base station 2 is the best choice to take over the call, so it allocates a traffic channel (TCH) to this station and the station acknowledges (events 7 and 8). Next, the MSC sends a handover order message to base station 1, which sends a similar message to the mobile unit (events 9 and 10). The message in event 10 notices the mobile station of the new channel assignment, as well as the power level to be used in the new cell. With the confirmations (event 11 and 12), the mobile station receives base station 2's SAT message and

regenerates this SAT message back to the base station (events 13 and 14). This continuity check is sufficient for base station 2 to confirm the handover (event 15) to the MSC [7].

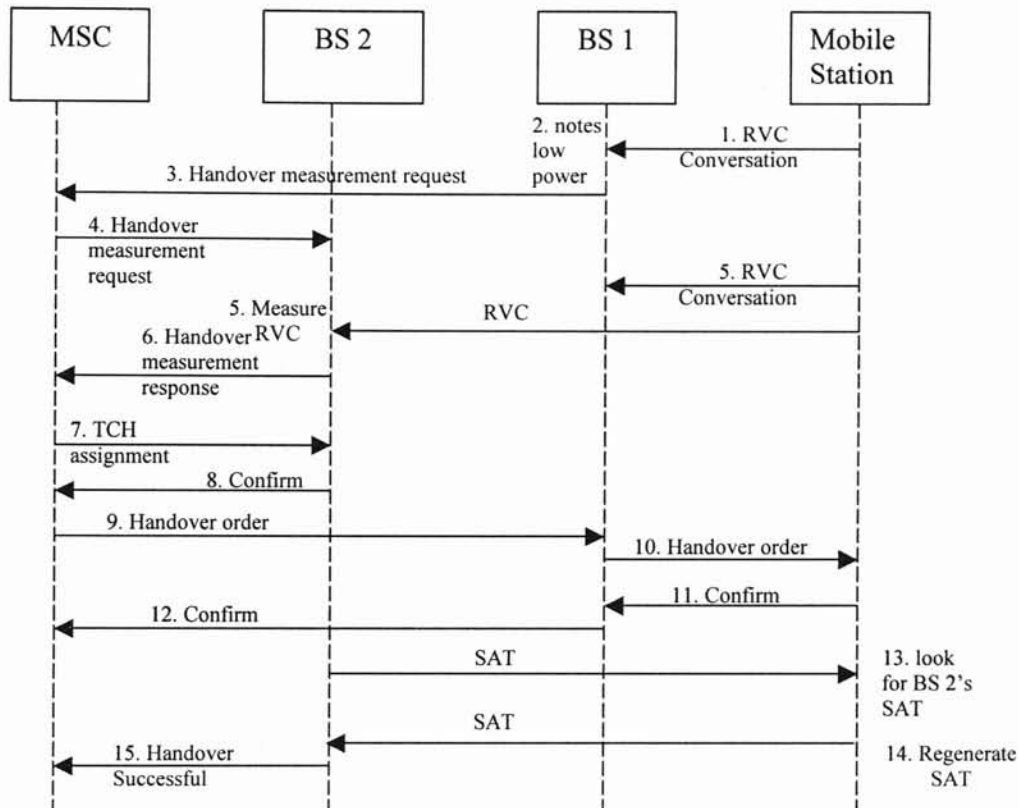


Figure 2-2. Handover Operation.

2.2.2 Handover for the second generation wireless communication systems

Figure 2-3 shows an example of how a mobile user can roam from cell-to-cell and how the system keeps a record of the mobile user's location, a function called mobility management. Upon the mobile station crossing a boundary, it sends a location update request (event 1), which contains its identification, to the base station (BS). In second generation systems, the mobile station monitors channels in other cells. In AMPS, the mobile station does not participate or make decisions about handover. If it finds a proper control channel in another cell that meets certain power and quality criteria, it notifies its serving base station by sending it a location update message. This message is then routed

to the new Visitor Location Register (VLR). The new VLR has no information about the entry for this user because the mobile user has already moved into its area [12].

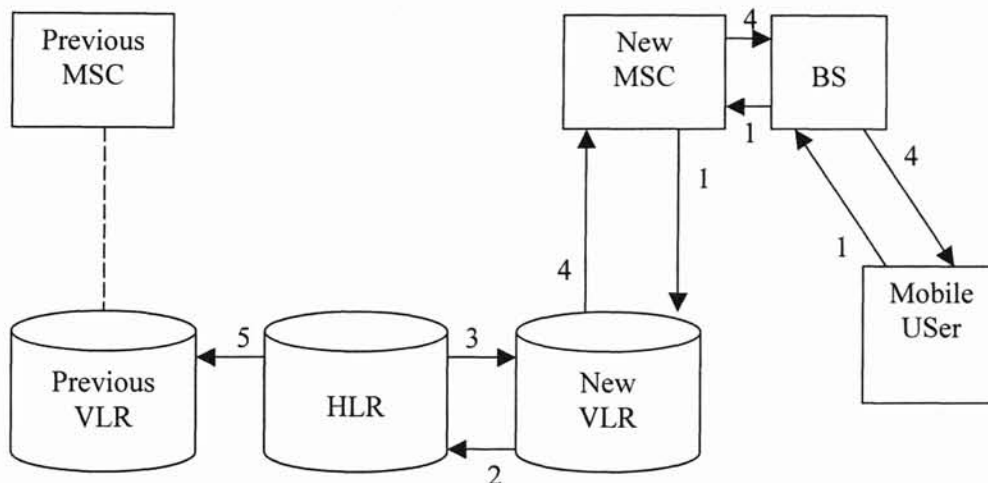


Figure 2-3. Mobility management operations.

The new VLR sends the query message to the user's home location register (event 2). This message includes the identity of the user as well as the identity of the new VLR that sent the message. In event 3, the HLR stores the subscriber's new location at the new VLR and then downline loads the user's subscription information to the new VLR. On receiving this information, the new VLR sends the acknowledgement of the location update through the new MSC to the MSC, and back to the originating mobile user (event 4). Finally, in event 5, the HLR sends a location cancellation message to the old VLR to clear the subscriber's data from its database. The mobile subscriber must be known only to one VLR at a time. In this example, when the subscriber has roamed to another area, the HLR has had to be updated. It can be seen that the HLR is the master of the subscriber data base and therefore coordinates changes to the VLRs as the subscriber roams through the cells. In the Pan-European Digital Cellular Standard, a handover margin parameter is used as the hysteresis margin [12]. The North American Personal Access Communications System (PACS) personal communication systems services standard combines the hysteresis margin with a dwell timer [13].

2.2.3 Mobile Assisted Handover (MAHO)

IS-54 B defines the mobile assisted handover, which is used to make the handover more efficient and faster. In this situation, the mobile station measures the quality of the forward traffic channel in relation to other channels emanating from other base stations [4]. It executes these procedures during idle times when not involved in sending or receiving traffic. The measurements taken by the mobile station are sent back to the base station. In turn, the base station uses this information to decide if handover is to be implemented. This modification to the traditional AMPS operation eliminates signaling substantially because neighboring cells do not have to measure the channel of the mobile station. IS-54 B is designed to support analog handover or digital handover as well as variations of analog-to-digital or digital-to-analog handovers. Even though the mobile station participates more in handover decisions than it did in the conventional AMPS, the operation is still controlled initially by the base station by directing the mobile station to send measurement messages back to the network. The message tells the mobile station which channels are to be monitored, measured, and reported upon.

2.2.3 CDMA Handover signaling

Soft handovers and hard handovers which use the same frequency assignment are originally initiated by the mobile station. The mobile station keeps searching for pilots to detect the existence of the CDMA channels and measure their signal strength. When the mobile station detects a pilot signal which is strong enough that is not associated with any of the forward traffic channels assigned to it, the following sequences will occur [14]:

- The mobile station sends a Pilot Strength Measurement Message to the base station, which lists the pilots received by the mobile station. This message initiates the handover process when the handover is initiated by the mobile station.
- The base station allocates a Forward Traffic Channel associated with that pilot, and then sends a Handover Direction Message to the mobile station and directs it to perform the

handover. For soft handovers, the Handover Direction Message lists multiple Forward Traffic Channels, some of which are already being demodulated by the mobile station. For hard handover, the Handover Direction Message lists one or more Forward Traffic Channels, none of which is currently demodulated by the mobile station.

- Following the execution of the Handover Direction Message, the mobile station sends a Handover Completion Message on the new Reverse Traffic Channel. This message serves the base station as a positive acknowledgement, indicating that the mobile station has successfully acquired the new Forward Traffic Channels.

2.2.4 Handover Parameters

There are three important reasons in soft handover to replace any additional base stations that can be detected by the mobile station as soon as possible [14]:

- Improved voice quality: cell boundaries usually offer poor coverage coupled with increased interference from other cells and therefore, forward traffic channel diversity from additional cells will improve the quality.
- Controlled mobile station interference: while on a boundary of a cell, the mobile station's interference to mobile stations in other cells is maximal and therefore, it is important to be able to power control it from these cells.
- Reduce call dropping probability: handover area in which the forward link is most vulnerable. A slow handover process coupled with a vehicle moving at high speed may cause the call to be dropped since the mobile station might no longer be able to demodulate the forward link transmitted from the original cell, losing the handover direction message.

2.2.5 Generalization of Handover

The studies of handover have taken place over a wide spectrum of scenarios. There are many situations, such as "small" or "large" cells, hard or soft handovers, and in wireless telephone or data networks. The scenarios vary with the random behavior of the propagation environment and the mobile user calls for a need to design various handover

properties that suit different situations. Each scenario presents its challenges. These challenges can be categorized [1]:

- Quality of service (call quality), or probability of outage
- Total number of handovers required to be performed as a mobile user moves between two adjacent base stations
- Reduce the number of unnecessary handovers, which happens in cases where remaining connected to the current base station is the best option in sustaining the communication link
- Minimize the delay in making handover, which is often computed as the distance between the cell boundary and the crossover point. The handover cross over point is defined with regards to the reception signal power drop (normally 3 dB) or as the point at which the probability of being assigned to the current base station drops below 0.5 [15]

These challenges are primarily based on the uses of the wireless system and the environments that the systems operate in. Microcells are prone to handover delays, whereas wireless voice and data networks have to consider traffic load for designing a handover algorithm because the handovers seriously influence the network performance. In urban situations with many antennas, high buildings are placed lower than the surrounding skyline and the user can experience deep fades as it turns around the corner of a building [16].

2.2.6 Types of Handover

The mobile station supports the following two handover procedures during a call [14]:

- Soft handover: A handover in which the mobile user commences communications with the approaching base station without interrupting communications with the current base station. Since mobile cellular phones typically contain a single radio, soft handovers can only be used between CDMA channels having identical frequency assignments. The operation is illustrated in Figure 2-4.

- **Hard Handover:** A handover in which the mobile station is transitioned between disjoint and adjacent sets of base stations, different frequency assignments, or different frame offsets. As depicted in Figure 2-5, continuity of the radio link is not maintained during hard handovers.

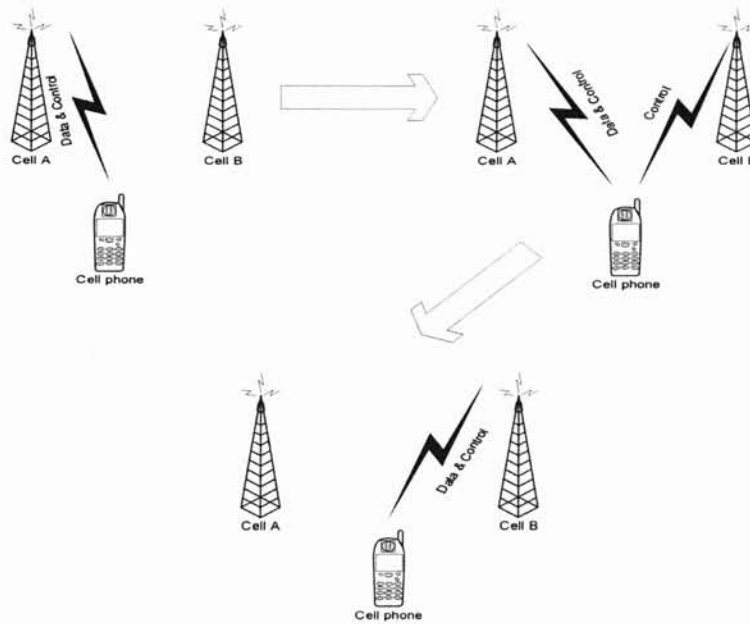


Figure 2-4. Soft Handover: In the soft handover process, the communication link with the mobile station is maintained at all times.

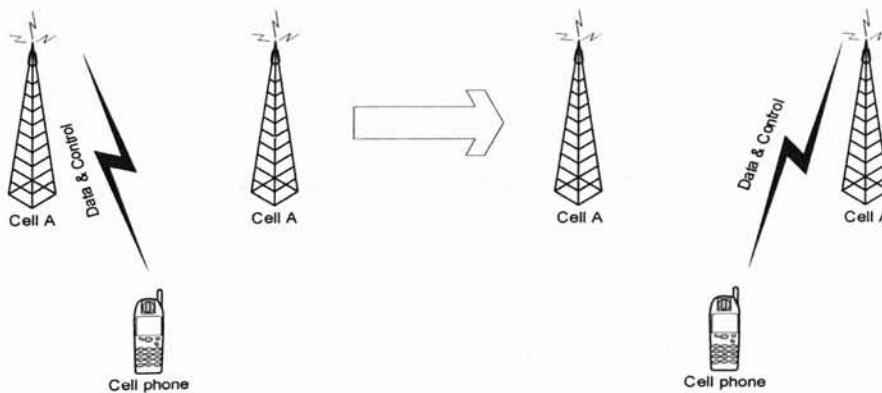


Figure 2-5. Hard handover: In the hard handover process, the communication link with the mobile station is momentarily disrupted.

2.2.7 Handover Scenario and Conventional Methods

The handover scenario consists of a mobile user which is moving between two adjacent base stations. Let the mobile user be moving away from its current base station A and towards the other base station B . These two base stations are the two from which the mobile system is likely to have the strongest received signal and are the closest ones.

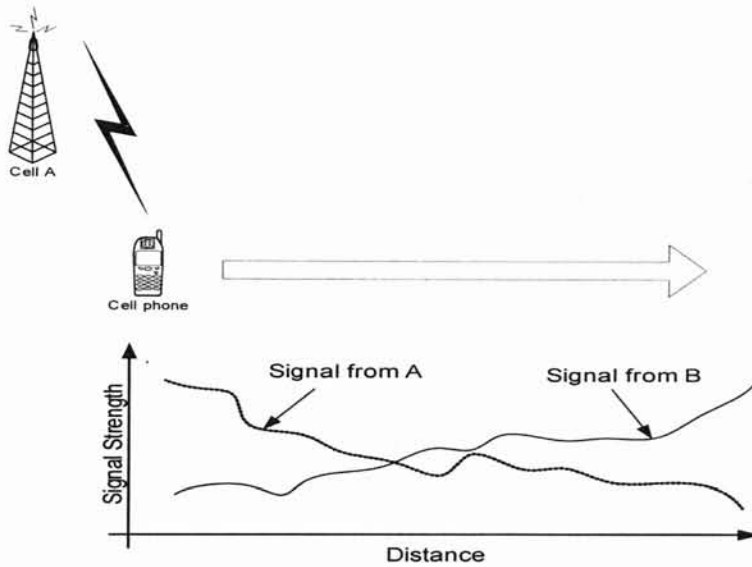


Figure 2-6. Signal strength vs. distance when user is moving from Cell A to Cell B .

The handover decision has to be made based upon a limited amount of information which is available to the mobile user and the base station at each time instant. This information includes signal strength measurements, mobile to base station distance [1, 16], bit error rate, and carrier to interference (C/I) ratio. Here we assume that the received signal is filtered such that the multipath fading effects can be neglected. The received signal power X (dB) at the k th time instant and the i th base station can be given by [1]

$$X_k^i = \mu - \eta \log_{10} d_k^i + Z_k^i \quad (2.1)$$

where μ is a function of the base station transmitter power, η is the path loss exponent associated with the simplified path loss model, d is the distance between the mobile user and the base station, and Z is the variance due to shadowing.

2.2.8. Received Signal Strength

A handover decision to the base station B is made from the current base station A when the average received signal power from base station B is stronger than the signal power received at base station A . Representing this in an inequality format we obtain

$$r^B[k] > r^A[k] \quad (2.2)$$

in which $r[k]$ is obtained from

$$r[k] = \frac{1}{N} \sum_{i=k-N+1}^k P_i \quad (2.3)$$

where P is the power [W] and N is the number of the samples. This strategy chooses the strongest signal at a given time. The decision is mainly based upon an averaged measurement of the received signal. This technique is to activate too many unnecessary handovers [12].

2.2.9. Relative Signal Strength with Hysteresis

A handover decision is made from the current base station A to B when

$$r^B[k] > r^A[k] + H \quad (2.4)$$

where H is the hysteresis margin. This technique provides a user to do a handover if and only if the new base station signal is sufficiently stronger than the current serving base station signal [17]. This method prohibits excessive ‘ping pong’ between two base stations [18].

2.2.10. Relative Signal Strength with Hysteresis and Threshold

A handover decision is made from the current serving station A to B when

$$r^B[k] > r^A[k] + H \text{ and } r^A[k] < T_c \quad (2.5)$$

where H is the hysteresis margin and T_c is a threshold value. This technique provides a user to conduct a handover to a new base station only if the current serving station’s signal level drops lower than a threshold and the target base station is stronger than the current one by a predefined hysteresis threshold value [17].

2.3 Dual array antenna system

Recently, Multi-Input Multi-Output (MIMO) technology based dual antenna array (DAA) systems have gained much attention due to their enormous spectral efficiency. Fochini and Gans demonstrated that DAA systems employing multiple antennas both at the transmitter and the receiver sites can obtain linearly increased channel capacity based on the number of antennas applied [32].

In this section, we provide an overview of DAA systems.

2.3.1 Information channel capacity of conventional communication system

The information theory gives an upper bound of the achievable information channel capacity, i.e., spectral efficiency. The information channel capacity over an AWGN channel is expressed by the well-known Shannon's formula [33]:

$$C = \log_2(1 + \rho), \quad [\text{bps/Hz}] \quad (2.6)$$

where ρ is SNR at the receiver. Many attempts have been conducted to increase the spectral efficiency using technologies such as channel coding, diversity schemes [34]. Among these efforts to increase the spectral efficiency, diversity schemes enable one to take advantage of the redundant information in replicas of the same information transmitted over independent fading channels to alleviate fading effects. Conventionally, diversity schemes have been studied in frequency, temporal, and spatial domains at the received signal. Especially, receiver diversity using multiple antennas is commonly used at the base station during the uplink duty cycles in mobile cellular systems.

Recently, the use of DAAs employing multiple antennas at the transmitter and receiver has been investigated in [32] and [35]. Especially, in [32], it was shown that the information channel capacity of a DAA system is increased linearly as the number of antenna elements at the transmitter and receiver are increased; provided that a rich scattering environment ensures the channel path gains between the transmit antenna elements and the receiver antenna elements such that they are uncorrelated. Although there have been many studies of the channel capacity of multiple antennas systems, the DAA system has the unique feature in the sense that multiple antenna elements are employed both at the transmitter and receiver; and a number of symbols are transmitted

in parallel through the multiple antennas at the transmitter, which enables DAA systems to achieve a high spectral efficiency.

2.3.2 Information Channel Capacity of DAA System

Foschini and Gans investigated the information channel capacity of DAA systems [32]. They showed that the capacity of independent fading MIMO channels is increased linearly, while the capacity of receiver diversity system applying an optimum combining single-input multi-output (SIMO) topology is increased logarithmically.

Shannon's formula for DAA systems can be generalized to [37]

$$C = B \log_2 \det \left(\mathbf{I} + \frac{P_T}{M\sigma^2} \mathbf{H} \cdot \mathbf{H}^* \right) \quad (2.7)$$

where B is the bandwidth, P_T is the total transmit power at the transmit site, M is the number of antenna at transmitter, N is the number of antenna at receiver, \mathbf{I} is identity matrix, the subscript $*$ represents conjugate transpose. \mathbf{H} is a complex channel gain matrix, which is defined as

$$\mathbf{H} = \begin{bmatrix} h_{11} & \dots & h_{1M} \\ \vdots & \ddots & \vdots \\ h_{N1} & \dots & h_{NM} \end{bmatrix} \quad (2.8)$$

In Eq. (2.8), h_{ij} is the complex channel path gain from the j th transmit antenna element to the i th receive antenna element, which is expressed as:

$$h_{ij} = \alpha_{ij} \cdot e^{j\phi_{ij}}, \quad (2.9)$$

where α_{ij} is the envelop of h_{ij} , which is a Rayleigh random variable, and ϕ is the phase of h_{ij} , which is uniformly distributed over 0 to 2π . Note that the bold capital letter represents a matrix.

In [32], the authors investigated the capacity of a communication link under a scattering multipath environment, which reflects the small-scale fading phenomenon only. However, the actual received signal in a cellular environment is not only impaired by

multipath fading but also severely attenuated by surrounding buildings and other large scale obstacles, known as the shadowing phenomenon. In [36], Lozano *et al.* analyzed the channel capacity of DAA systems under composite Rayleigh fading and lognormally shadowed wireless environments. Considering shadowing, the squared-envelop of the complex path gain between the j th transmit antenna element and the i th receiver antenna element becomes:

$$|h_{ij}|^2 = \alpha_{ij}^2 \cdot \Omega_{ij}, \quad (2.10)$$

where Ω represents the squared-envelop of the complex path gain due to the shadowing modeled by the lognormal distributed random variable. Note that the mean value of Ω depends on the distance between the transmitter and the receiver. It is well known that the received signal power decays with a function of distance between a transmitter and a receiver. Excluding the shadowing and fading phenomena, the received power just considering signal attenuation which is referred to as the local-average power becomes [37]

$$L = [4 \cdot 10^{-14} \cdot d^{-3.5} \cdot G] = [-134 - 35 \log_{10}(d) + 10 \log_{10}(G)] \text{ dB} \quad (2.11)$$

where d is the distance in kilometers between a transmitter and a receiver and G is antenna gain in dBi. In (2.10), the probability density function of the squared-envelop of the complex path gain due to shadowing is given by:

$$f_{\Omega}(\Omega) = \frac{\zeta}{\sigma_{\Omega} \cdot \Omega \sqrt{2\pi}} \exp\left(-\frac{(\zeta \ln(\Omega) - L)^2}{2\sigma_{\Omega}^2}\right) \quad (2.12)$$

where $\zeta = 10/\ln 10 = 4.3429$, L is local average power given as Eq. (2.11), and σ_{Ω}^2 is the variance of the lognormal random variable Ω . The correlation among the entries of the channel gain matrix \mathbf{H} is determined by the antenna spacing and angle spread. We assume each antenna element is spaced far apart such that each signal propagation path is uncorrelated to each other. Therefore, the rows of \mathbf{H} are always independent, whereas the columns can be either linearly dependent or independent.

2.3.3.1 Steered Directive Array System

Let us first consider the following steered directive array antenna system illustrated in Figure 2-7. As shown in the figure, the M closely spaced antennas operate coherently at the base station. Each base station antenna has a gain of 15 dBi, while the terminal is equipped with a single omnidirectional antenna. Since the directive array antenna synthesizes narrower beam patterns as the number of antenna elements increase, more power can be launched to the direction of the mobile user, thereby increasing the received signal power at the receiver. Note that each antenna transmits identical information.

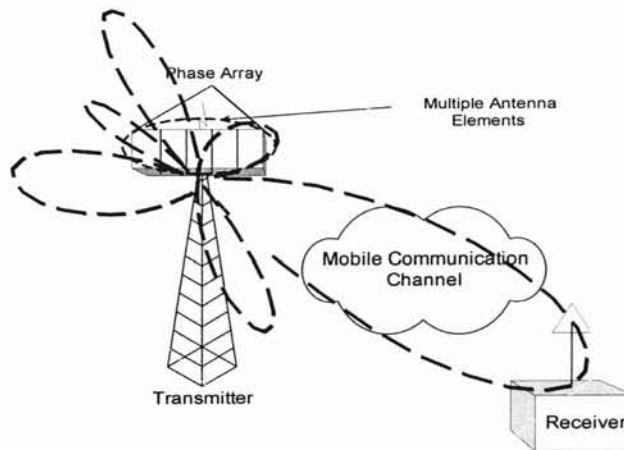


Figure 2-7. Illustration of the steered directive array system.

Since each antenna element of the directive array is closely located such that they operate coherently, the channel path gains from the individual elements are identical, i.e., $h_i = h$. Therefore, the capacity of the steered directive array antenna system can be obtained from (2.7)

$$C = B \log_2 \left(1 + \frac{MP_T |h|^2}{\sigma^2} \right), \quad (2.13)$$

where P_T is a transmit power at each element, thereby the total transmit power of directive array is MP_T . Especially, in broadband data communication systems, the peak

data rate supported for single user is of interest. This single user data rate can be evaluated from Eq. (2.13) assuming that the total available bandwidth B is dedicated to a single user.

Since the complex channel gain is a random variable, the capacity value also becomes a random variable. To evaluate the attainable capacity value for a given location, capacity outage is used. For example, the capacity supported in 90% of locations is plotted at a different distance, in Figure 2-8.

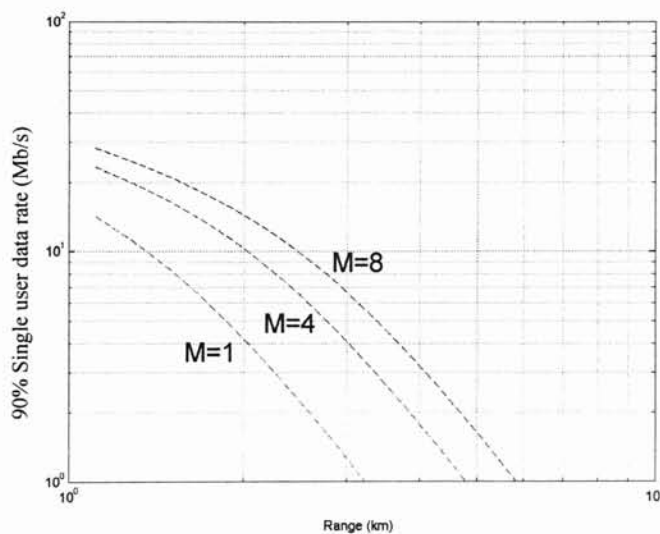


Figure 2-8. Single user data rate supported in 90% of locations vs. the range for the steered directive array antenna system.

2.3.3.2 Transmit diversity

In [38], Alamouti showed that the M -transmit diversity system provides the same diversity order as in M -receiver diversity system. Usually, the physical size of current mobile terminals tend to be smaller, while that of the base station is not relatively constrained. Thus, the major benefit of the transmit diversity scheme is the physical dimension of receiver is no longer a limitation to obtain diversity gain, since the gain can be obtained by employing additional antenna elements at the transmitter site. The system configuration is illustrated in Figure 2-9.

Transmit diversity systems employ M antenna elements at the transmitter site, as in the steered directive array antenna system. However, the antenna element spacing should be larger than that of steered direction array antenna system to ensure uncorrelated channel path gains from the individual transmit elements. Also, in the transmit diversity system the total transmit power is limited to P_T , regardless of number of antenna elements. Therefore, transmission power from each antenna elements is $\frac{P_T}{M}$.

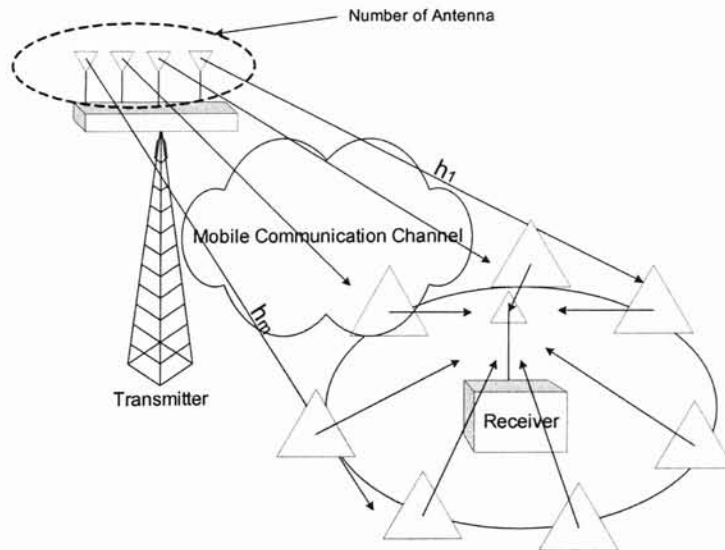


Figure 2-9. Illustration of the transmitter diversity system.

In transmit diversity system, the channel matrix of transmit diversity system is given as

$$\mathbf{H} = [h_1 \quad h_2 \quad \dots \quad h_M], \quad (2.14)$$

the capacity is now expressed from Eq. (2.7) as:

$$C = B \log_2 \left(1 + \frac{P_T}{M\sigma^2} \sum_{m=1}^M |h_m|^2 \right) \quad (2.15)$$

with h_m the complex channel gain from the m th transmit antenna element to a receiver antenna.

In Figure 2-10, single user data rate supported in 90% of locations is plotted versus the distance. Compared to the directive array antenna system, the capacity improvement is not noticeable. This is due to the fact that the total transmission power in the transmit diversity system is constrained. In other words, the total transmission power in a directive array antenna system is increased as the number of antenna elements increases, while that in transmit diversity system is limited as a constant regardless of the number of antenna elements. Although one drawback of allowing a system to increase its transmission power is that this results in a larger amount of cochannel interference for other systems and vice-versa, the interference experienced at this system also will become a considerable issue to the overall performance.

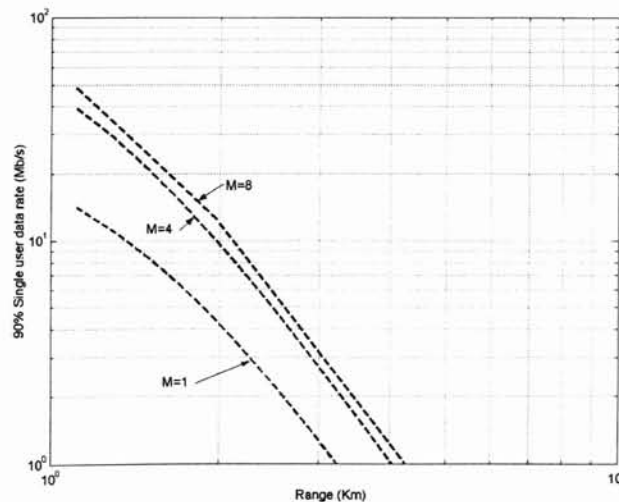


Figure 2-10. Single user data rate supported in 90% of locations vs. range (distance) for M -antenna transmit diversity at the base station and single antenna at the terminal.

2.3.3.3 Dual array antenna system

The last system analyzed here is the dual array antenna system. This system is illustrated in figure 2-11.

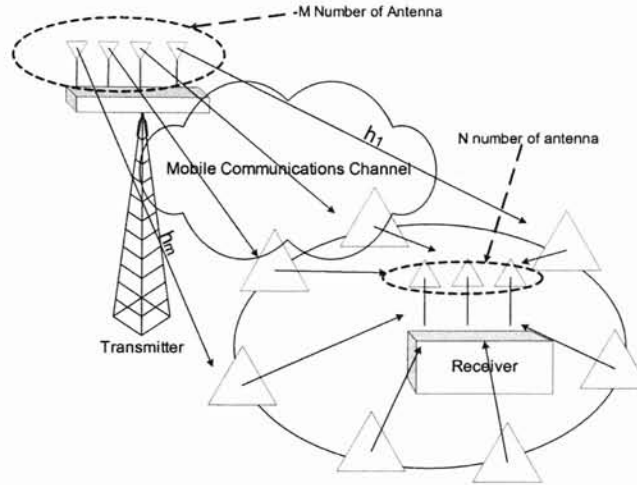


Figure 2-11. Multiple-input multiple-output (MIMO) topology.

In dual array systems, M antennas are employed at the transmitter site, while N antennas are employed at receiver site. For the convenience of illustration in the following equations, we set $M = N$ herein. As in transmit diversity systems the total transmission power is constrained to P_T .

For transmit diversity system, the channel gain matrix is given as:

$$\mathbf{H} = \begin{bmatrix} h_{11} & \dots & h_{1M} \\ \vdots & \ddots & \vdots \\ h_{M1} & \dots & h_{MM} \end{bmatrix} \quad (2.16)$$

Since each channel gain h_{ij} in \mathbf{H} is uncorrelated to each other, the covariance matrix of channel gain is diagonal matrix, i.e.:

$$\mathbf{H} \cdot \mathbf{H}^* = \begin{bmatrix} h_{11} \cdot h_{11}^* + h_{12} \cdot h_{12}^* + \dots + h_{1M} \cdot h_{1M}^* & 0 & 0 & \dots & 0 \\ 0 & \ddots & 0 & \dots & 0 \\ 0 & 0 & \ddots & \dots & 0 \\ 0 & 0 & 0 & \dots & h_{11} \cdot h_{11}^* + h_{21} \cdot h_{21}^* + \dots + h_{MM} \cdot h_{MM}^* \end{bmatrix} \quad (2.17)$$

Therefore, by substituting (2.17) into (2.7) we obtain the channel capacity equation as:

$$C = B \sum_{i=1}^M \log_2 \left(1 + \frac{P_T}{M\sigma^2} \sum_{j=1}^M |h_{ij}|^2 \right). \quad (2.18)$$

As shown in Figure 2-12, the channel capacity of the dual array antenna system grows linearly as the number of antenna increases. Thus, compared to the previous antenna system, enormous channel capacity gains can be obtained in DAA systems by adding additional antennas both at the transmitter and thereceiver sites.

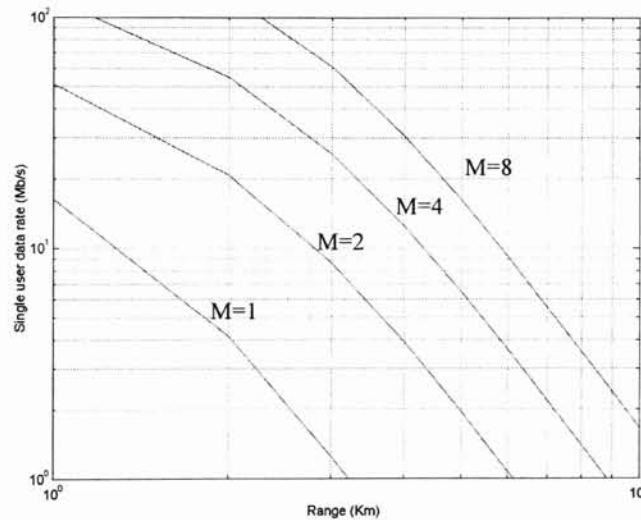


Figure 2-12. Single user data rate supported in 90% of locations vs. range (distance) for the dual array antenna system.

CHAPTER III

Intelligent Handover Control Technologies

This chapter analyzes and proposes fuzzy logic and artificial neural network (ANN) algorithm to enable multi variable optimization in the handover decision procedure.

The rest of this chapter is organized as follows. Section 3.1 presents the proposed handover management algorithm for mobile communication networks and also provides an overview of fuzzy logic and how it can be implemented to assist handover procedures. Section 3.2 provides a review of the learning vector quantization (LVQ) ANN technology that could be used for multivariable control of handover operations. Section 3.3 provides the handover procedure for IMT-2000 and its specifications.

3.1 Handover Management

In mobile communication systems, the most common factor to initiate handover is when the signal to noise ratio or received signal power is less than a predefined threshold value [20]. The next generation communication environment will enable different mobile network systems to interoperate with each other and provide mobile network service.

By the seamless tracking of the subscriber's information, such as quality of service, signal strength, bit error rate, and signal to noise ratio, an improved handover algorithm that could utilize these different handover parameters could be developed.

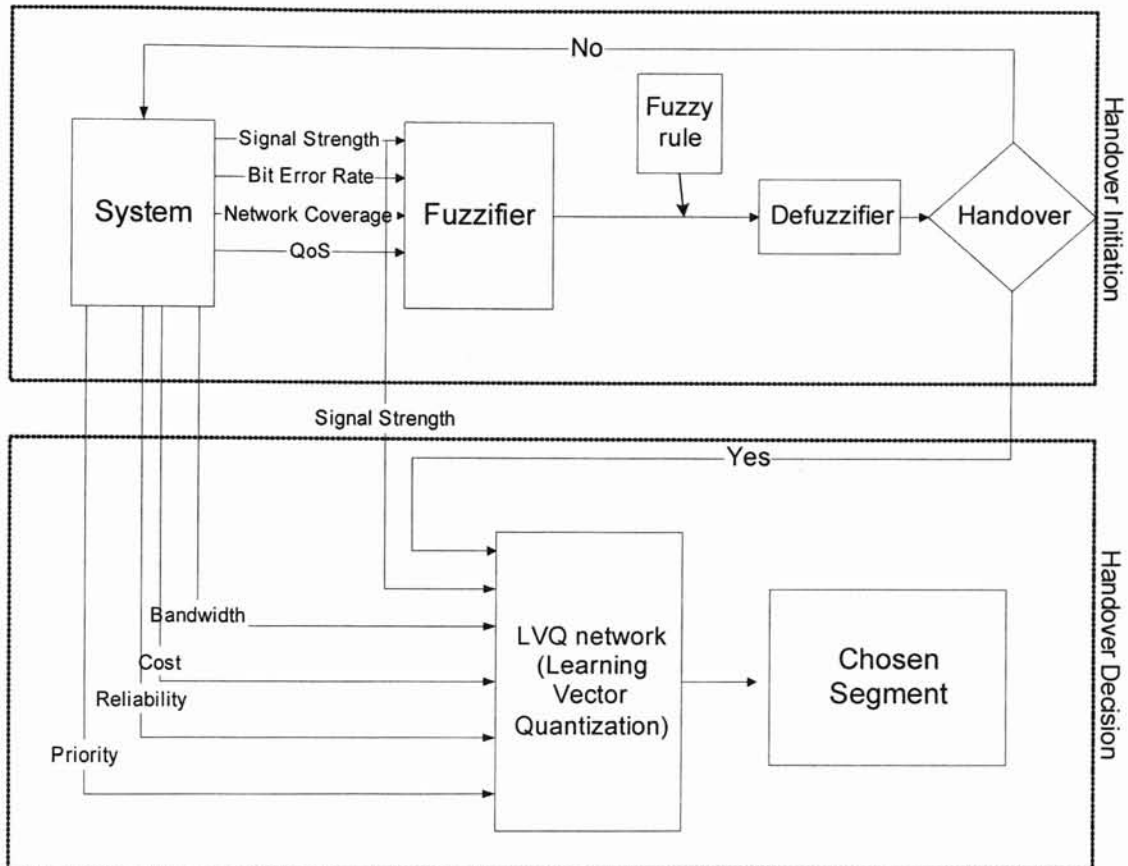


Figure 3-1. Block diagram of a proposed example Fuzzy Logic and LVQ Network handover algorithm.

For handover initiation, four different factors could be used: signal strength, bit error rate, network coverage, and quality of service [20]. These factors may be changed depending on the characteristics of the system. Three basic operation stages exist. In the first stage, the parameters of the system are fed into the fuzzier, which will transform the parameters into fuzzy sets which make membership sets. The second stage is to apply a fuzzy rule, which is defined as a set of If-Then function. Following this set of rules an intelligent handover decision could be made.

The major objective of the handover decision algorithm is to select a decision plane serving segment. The example control system block diagram will be explained in the following chapters.

3.1.1 Problem Description

‘Inherent uncertainty’ refers to the property of a situation such that knowing the outcome of the situation does not allow us to make an exact decision about the situation. A well-known example is the judgment of the person’s weight. Although the weight of a person is measured exactly, the question “Is that person heavy?” cannot be answered without some uncertainty. A threshold could be used such that if the person’s weight exceeds a certain threshold then the person could be included into the set of heavy people, otherwise the person is excluded. However, to choose such a threshold is not simple. In mobile communications, the received signal strength (RSS) and MS-BS distance fall into this category of uncertainty because it is difficult to define thresholds at which the system can determine whether there is enough power or whether the mobile is close enough. Conventional methods use thresholds, and at the same time try to compensate for the sharpness of the threshold by allowing a hysteresis margin. By adapting fuzzy logic, the threshold value is smoothed out. An output parameter HO_Factor makes an important recommendation for a handover to the other base station depending on its value which lies in the range between 0 and 1. The value indicates the strength of the recommendation. If the indication is strong, the request to handover to the adjacent base station is strong, and so HO_Factor is high.

3.1.2 Fuzzy Logic Method

Fuzzy logic uses partial membership in a set, and the degree to which elements belongs in the set is determined by the membership function of the fuzzy set. The membership μ_A function takes in some value as an output value between 0 and 1 [16].

$$\mu_A : X \rightarrow [0,1] \quad (3.1)$$

The membership function value is known as the degree of membership or the truth value. So if the system takes in two different kinds of inputs, a set of membership functions, the range of input values, and the type of function are a matter of designing choice. Suppose a measurement from each kind of input is taken, then the truth value of each kind of input is obtained. The truth value enables the input to be mapped to the output using a set of rules [20]. The rule is **IF** <input variables belong to some specific set> **then** <output

variable belongs to some specific set>. An example can be if the input variable is weight and height, and the output is size, then **If** weight is ‘medium’ **and** height is ‘tall’, **then** size is ‘medium.’ The truth value of size ‘medium’ is simply the minimum of the truth value of height in the set ‘tall’ and weight in the set ‘medium.’ That is,

$$\mu_{\text{size, medium}} = \min [\mu_{\text{height, tall}}, \mu_{\text{weight, medium}}] \quad (3.2)$$

In this case the ‘and’ operator is used, but if the ‘or’ operator is used, then the maximum of the truth values is taken. After the truth values of all the rules are taken, they are plotted against the possible values of the output.

3.1.3. Fuzzy Logic Solution

In [16], the fuzzy sets are used for the RSS measurements, MS-BS distance measurements, and the HO_Factor. The membership functions are simple triangular functions which are similar for all three domains. For RSS measurements x , in the range [-80, -20] dBm, the membership functions can be defined as [38]:

$$\begin{aligned} \mu_{RSS,weak}(x) &= \left\{ \begin{array}{l} 1, \text{ if } x \leq -65 \\ \frac{(-50-x)}{15}, \text{ if } -65 < x < -50 \\ 0, \text{ if } x \geq -50 \end{array} \right\} \\ \mu_{RSS,medium}(x) &= \left\{ \begin{array}{l} 0, \text{ if } x \leq -65 \\ \frac{(x+65)}{15}, \text{ if } -65 < x < -50 \\ \frac{(-35-x)}{15}, \text{ if } -50 < x < -35 \\ 0, \text{ if } x \geq -35 \end{array} \right\} \\ \mu_{RSS,strong}(x) &= \left\{ \begin{array}{l} 0, \text{ if } x \leq -50 \\ \frac{(x+50)}{15}, \text{ if } -50 < x < -35 \\ 1, \text{ if } x \geq -35 \end{array} \right\} \end{aligned} \quad (3.3)$$

variable belongs to some specific set>. An example can be if the input variable is weight and height, and the output is size, then **If** weight is ‘medium’ **and** height is ‘tall’, **then** size is ‘medium.’ The truth value of size ‘medium’ is simply the minimum of the truth value of height in the set ‘tall’ and weight in the set ‘medium.’ That is,

$$\mu_{\text{size, medium}} = \min [\mu_{\text{height, tall}}, \mu_{\text{weight, medium}}] \quad (3.2)$$

In this case the ‘*and*’ operator is used, but if the ‘*or*’ operator is used, then the maximum of the truth values is taken. After the truth values of all the rules are taken, they are plotted against the possible values of the output.

3.1.3. Fuzzy Logic Solution

In [16], the fuzzy sets are used for the RSS measurements, MS-BS distance measurements, and the HO_Factor. The membership functions are simple triangular functions which are similar for all three domains. For RSS measurements x , in the range $[-80, -20]$ dBm, the membership functions can be defined as [38]:

$$\begin{aligned} \mu_{RSS,weak}(x) &= \begin{cases} 1, & \text{if } x \leq -65 \\ \frac{-50-x}{15}, & \text{if } -65 < x < -50 \\ 0, & \text{if } x \geq -50 \end{cases} \\ \mu_{RSS,medium}(x) &= \begin{cases} 0, & \text{if } x \leq -65 \\ \frac{(x+65)}{15}, & \text{if } -65 < x < -50 \\ \frac{(-35-x)}{15}, & \text{if } -50 < x < -35 \\ 0, & \text{if } x \geq -35 \end{cases} \\ \mu_{RSS,strong}(x) &= \begin{cases} 0, & \text{if } x \leq -50 \\ \frac{(x+50)}{15}, & \text{if } -50 < x < -35 \\ 1, & \text{if } x \geq -35 \end{cases} \end{aligned} \quad (3.3)$$

and plots of this membership functions are illustrated in figure 3.2.

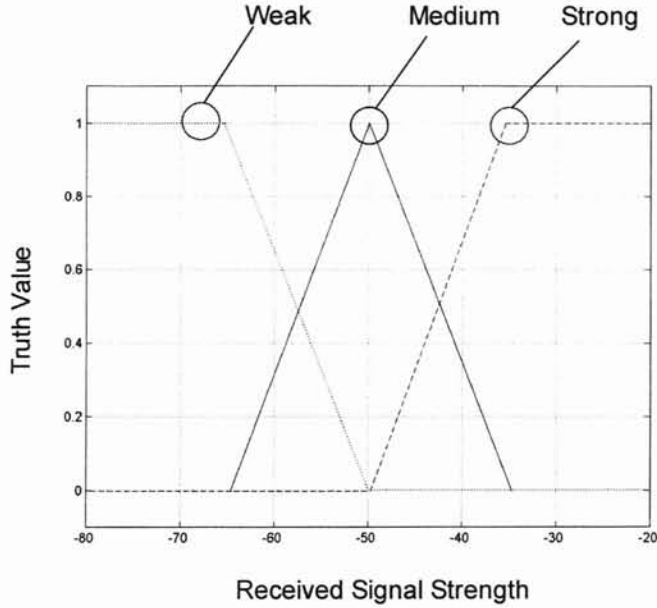


Figure 3.2 Fuzzy sets of the RSS.

For the MS-BS distance measurements d over the specific interval $[0, 500]$ m, the membership functions could be set as [38]:

$$\mu_{Dis, near}(d) = \begin{cases} 1, & \text{if } d \leq 125 \\ \frac{(250-d)}{125}, & \text{if } 125 < d < 250 \\ 0, & \text{if } d \geq 250 \end{cases}$$

$$\mu_{Dis, medium}(d) = \begin{cases} 0, & \text{if } d \leq 125 \\ \frac{(d-125)}{125}, & \text{if } 125 < d < 250 \\ \frac{(375-d)}{125}, & \text{if } 250 < d < 375 \\ 0, & \text{if } d \geq 375 \end{cases}$$

$$\mu_{Dis, far}(d) = \begin{cases} 0, & \text{if } d \leq 250 \\ \frac{(d-250)}{125}, & \text{if } 250 < d < 375 \\ 1, & \text{if } d \geq 375 \end{cases} \quad (3.4)$$

and plots of this membership functions is illustrated in Figure 3.3.

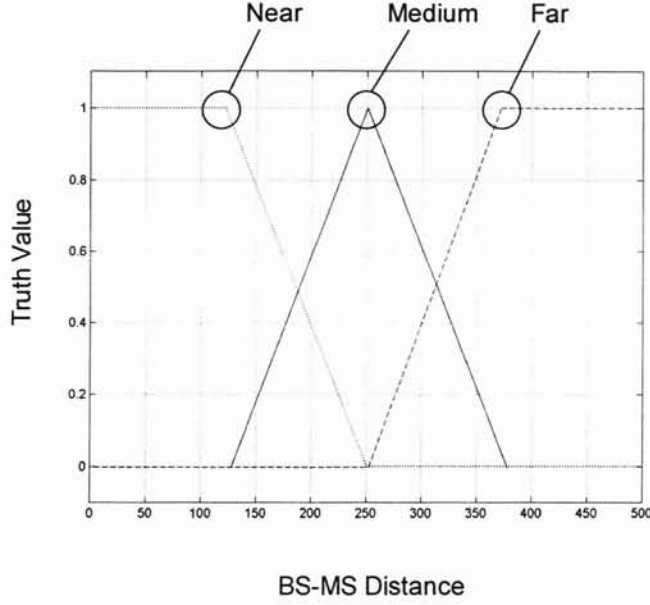


Figure 3.3 Fuzzy sets of the distance between base station and mobile station.

For the output parameter HO_Factor h over the given time interval $[0, 1]$, the membership functions are defined as [38]:

$$\mu_{ho,low}(h) = \begin{cases} 1, & \text{if } h \leq 0.25 \\ \frac{(0.5-h)}{0.25}, & \text{if } 0.25 < h < 0.5 \\ 0, & \text{if } h \geq 0.5 \end{cases}$$

$$\mu_{ho,medium}(h) = \begin{cases} 0, & \text{if } h \leq 0.25 \\ \frac{(h-0.25)}{0.25}, & \text{if } 0.25 < h < 0.5 \\ \frac{(0.75-h)}{0.25}, & \text{if } 0.5 < h < 0.75 \\ 0, & \text{if } h \geq 0.75 \end{cases}$$

$$\mu_{ho,high}(h) = \begin{cases} 0, & \text{if } h \leq 0.5 \\ \frac{(h-0.5)}{0.25}, & \text{if } 0.5 < h < 0.75 \\ 1, & \text{if } h \geq 0.75 \end{cases} \quad (3.5)$$

and plots of these membership functions are illustrated in figure 3.4.

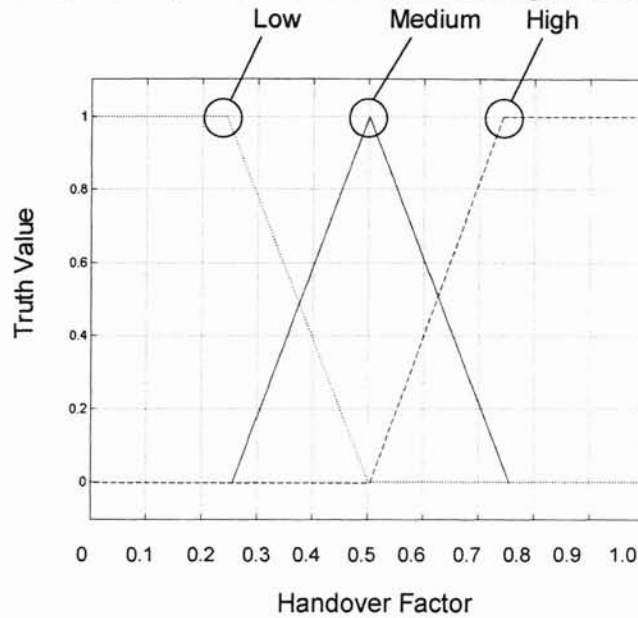


Figure 3.4 Fuzzy sets of Handover factor.

The following set of fuzzy rules can be used to decide the output [38]:

- IF** RSS is weak **and** MS-BS Distance is near, **then** HO_Factor is medium.
- IF** RSS is weak **and** MS-BS Distance is medium, **then** HO_Factor is high.
- IF** RSS is weak **and** MS-BS Distance is far, **then** HO_Factor is high.
- IF** RSS is medium **and** MS-BS Distance is near, **then** HO_Factor is low.
- IF** RSS is medium **and** MS-BS Distance is medium, **then** HO_Factor is medium.
- IF** RSS is medium **and** MS-BS Distance is far, **then** HO_Factor is high.
- IF** RSS is strong **and** MS-BS Distance is near, **then** HO_Factor is low.
- IF** RSS is strong **and** MS-BS Distance is medium, **then** HO_Factor is low.
- IF** RSS is strong **and** MS-BS Distance is far, **then** HO_Factor is medium.

These rules can be summarized into the following Table 4.

HO_Factor		RSS		
		Weak	Medium	Strong
MS-BS Distance	Near	Medium	Low	Low
	Medium	High	Medium	Low
	Far	High	High	Medium

Table 4. Rule of Fuzzy sets.

As an example, suppose that RSS indicates $x = -40$ dBm, and that the MS-BS distance $d = 350$ m, then we obtain

$$\mu_{RSS,Weak}(-40) = 0 \qquad \mu_{Dist,near}(350) = 0 \qquad (3.6)$$

$$\mu_{RSS,medium}(-40) = \frac{1}{3} \qquad \mu_{Dist,medium}(350) = \frac{1}{5} \qquad (3.7)$$

$$\mu_{RSS,Strong}(-40) = \frac{2}{3} \qquad \mu_{Dist,Far}(350) = \frac{4}{5} \qquad (3.8)$$

The HO_Factor can be evaluated by using the min-max equation,

$$\mu_{HO_Factor,low}(h) = \max \left[\min \left(\frac{1}{3}, 0 \right), \min \left(\frac{2}{3}, 0 \right), \min \left(\frac{2}{3}, \frac{1}{5} \right) \right] = \frac{1}{5}, \quad 0 \leq h \leq 0.5 \qquad (3.9)$$

$$\mu_{HO_Factor,medium}(h) = \max \left[\min(0, 0), \min \left(\frac{1}{3}, \frac{1}{5} \right), \min \left(\frac{2}{3}, \frac{4}{5} \right) \right] = \frac{2}{3}, \quad 0.25 \leq h \leq 0.75 \qquad (3.10)$$

$$\mu_{HO_Factor,high}(h) = \max \left[\min \left(0, \frac{1}{5} \right), \min \left(0, \frac{4}{5} \right), \min \left(\frac{1}{3}, \frac{4}{5} \right) \right] = \frac{1}{3}, \quad 0.5 \leq h \leq 1 \qquad (3.11)$$

This result is illustrated in Figure 3.5.

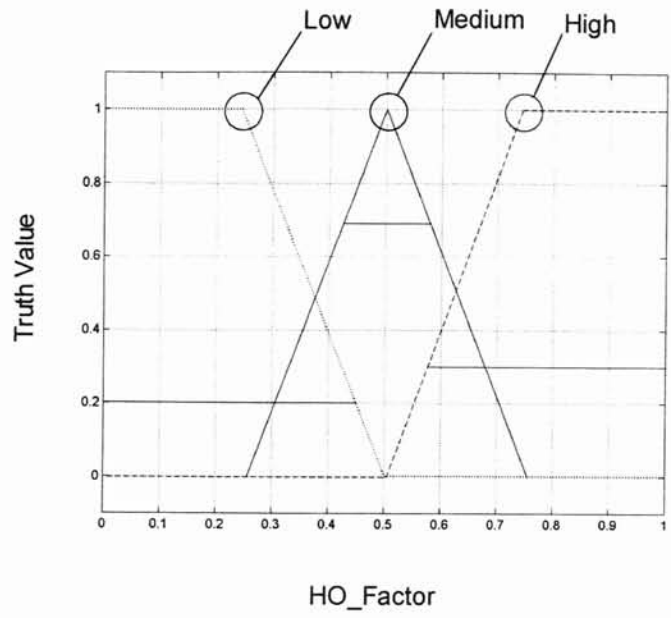


Figure 3.5 Result of the min-max equations.

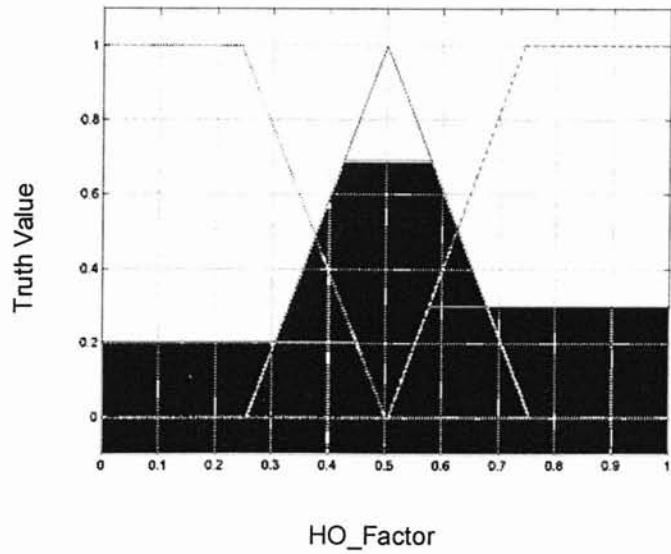


Figure 3.6 Result of the fuzzy logic sets.

In order to find a value for the HO_Factor output measurement, the plot of all output values against all possible values of the output is used.

Therefore, in this case (RSS = -40 dBm, MS-BS distance = 350 m), the HO_Factor value can be obtained by using the centroid algorithm [1].

$$\text{HO_Factor} = 0.37425$$

Because the HO_Factor is lower than 0.5 [15], handover operation is not initiated.

3.2. Pattern Recognition by Artificial Neural Network

3.2.1. Basic Property of Learning Vector Quantization (LVQ)

Among the different neural network architectures the learning vector quantization (LVQ) has been recognized for its superiority in pattern recognition to its counterparts such as multilayer perceptron [21], and therefore LVQ is used as an example to assist the multivariable controlled handover process. The LVQ network is a hybrid network and it uses both supervised and unsupervised learning to form classifications [22]. In the LVQ network, each neuron in the first layer is assigned for a class, with several neurons often assigned to the same class. Each class is assigned to one neuron in the second layer. The number of neurons in the first layer, S^1 , will therefore always be at least as large as the number of neurons in the second layer, S^2 , and will usually be larger. A block diagram of the LVQ network is illustrated in figure 3.7.

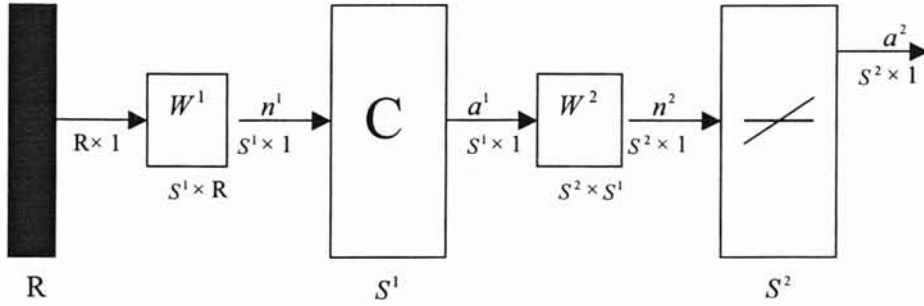


Figure 3.7. Block diagram of LVQ network

In Fig.3.7, R indicates the number of input vector, a is the output of each layer, n is the net input, W is the weight matrix, and C represents competition function

As with the competitive network, each neuron in the first layer of the LVQ network learns a prototype vector, which allows it to classify a region of the input space. However, instead of computing the proximity of the input and weight vector by using the inner product [21], we can obtain the net input.

The net input of the first layer of the LVQ will be

$$n_i^1 = -\|_i w^1 - p\| \quad (3.12)$$

Or, in vector form,

$$n^1 = - \begin{bmatrix} \|_1 w^1 - p\| \\ \|_2 w^1 - p\| \\ \vdots \\ \|_{S^1} w^1 - p\| \end{bmatrix} \quad (3.13)$$

The output of the first layer of the LVQ is

Acct # 1-1-70100-2460

SSN:

Name:

DATE	DAY	IN	OUT	IN	OUT	IN	OUT	IN	OUT	Hours Worked	Time Reported*
12	SA										
13	SU										
14	MO										
15	TU	8:45	4:45							8.0	
16	WE										
17	TH										
18	FR										
* Minutes Converted to Decimals										TOTAL	

Student Signature: _____ Supervisor's Signature: _____

DATE	DAY	IN	OUT	IN	OUT	IN	OUT	IN	OUT	Hours Worked	Time Reported*
19	SA										
20	SU										
21	MO										
22	TU										
23	WE	9:00	3:30							6.5	
24	TH	9:00	5:00							8.0	
25	FR										
* Minutes Converted to Decimals										TOTAL	14.5

Student Signature: _____ Supervisor's Signature: _____

DATE	DAY	IN	OUT	IN	OUT	IN	OUT	IN	OUT	Hours Worked	Time Reported*
26	SA										
27	SU										
28	MO										
29	TU										
30	WE	9:00	11:00							2.0	
01	TH	11:45	5:00							5.25	
02	FR										
* Minutes Converted to Decimals										TOTAL	7.25

Student Signature: _____ Supervisor's Signature: _____

DATE	DAY	IN	OUT	IN	OUT	IN	OUT	IN	OUT	Hours Worked	Time Reported*
3	SA										
4	SU										
5	MO	9:00	5:00							8.0	
6	TU										
7	WE										
8	TH										
9	FR										
* Minutes Converted to Decimals										TOTAL	8.0

Student Signature: _____ Supervisor's Signature: _____

Acct # 1-1-70100-2460

SSN:

Name:

DATE	DAY	IN	OUT	IN	OUT	IN	OUT	IN	OUT	Hours Worked	Time Reported*
10	SA										
11	SU										
12	MO										
13	TU										
14	WE										
15	TH	8:45	9:00	10:00						1.00 1.25	
16	FR	9:00								1.00	
* Minutes Converted to Decimals										TOTAL	1.00 1.25

Student Signature: _____ Supervisor's Signature: _____

DATE	DAY	IN	OUT	IN	OUT	IN	OUT	IN	OUT	Hours Worked	Time Reported*
	SA										
	SU										
	MO										
	TU										
	WE										
	TH										
	FR										
* Minutes Converted to Decimals										TOTAL	

Student Signature: _____ Supervisor's Signature: _____

DATE	DAY	IN	OUT	IN	OUT	IN	OUT	IN	OUT	Hours Worked	Time Reported*
	SA										
	SU										
	MO										
	TU										
	WE										
	TH										
	FR										
* Minutes Converted to Decimals										TOTAL	

Student Signature: _____ Supervisor's Signature: _____

DATE	DAY	IN	OUT	IN	OUT	IN	OUT	IN	OUT	Hours Worked	Time Reported*
	SA										
	SU										
	MO										
	TU										
	WE										
	TH										
	FR										
* Minutes Converted to Decimals										TOTAL	

Student Signature: _____ Supervisor's Signature: _____

The second phase, which is shown in figure 3-11, is the format of transformation of the MU while it resides within the network boundary cell [23]. When BS 1 sends a Reconfiguration Begin (RECONFIG_beg) message to the MU, the format transformation is initiated. This message specifies the start of the download procedure. When the MU is ready to change to the new system, the MU returns a Reconfiguration Ready message to BS 1. When the network is ready for the new connection, SW 1 sends a Reroute Ready message to BS 1. Since the MU has activated a transmitter/receiver for each network, the MU is able to measure and compare signal strength for adjacent base stations for both systems. When handover to BS 2, which is the target base station is initiated, the MU sends an Intersystem Handover Required message to BS 1. BS 1 replies with a Reconfiguration Execute message to the MU, which triggers the MU to switch to network 2 operations. The MU sends the Reconfiguration Done message, and the MU is able to perform a network 2 handover to BS 2 [23].

3.3.3 Performance Evaluation

The additional signaling time (T_s) is the total time needed for transmission and processing of the messages of the intersystem handover protocol. T_s is calculated by summing the signaling time required for each of the steps [23]:

$$T_s = \sum_{i=1}^n T_i \quad (3.26)$$

The time to send a message (M_i) is calculated as:

$$M_i = \alpha_i + \beta_i + \gamma_i, \quad i = 1, \dots, 7, 9, \dots, 16 \quad (3.27)$$

where i is the number of steps for the handover, α_i is the transmission time, β_i is the propagation time, and γ_i is the processing time for the control message. The transmission time α_i is computed by :

$$\alpha_i = \frac{b_i}{R} \quad (3.28)$$

In [23], the mobile control handover (MCHO) case is considered and illustrated in figure 3-10. When the mobile user (MU) approaches the intersystem boundary cell, the mobile user can hear a beacon from the approaching network base station as well as the cell base station. When the handover is initiated, the mobile user or the network sends an intersystem handover warning (ISHO_warn) message to base station (BS) 1 which is the serving base station. The ISHO_warn message must contain the previous base station and identification of the mobile station. BS 1 sends an acknowledgement to the mobile station. BS 1 forwards the ISHO_warn message to switch (SW) 1. SW1 replies with an acknowledgement message to BS 1 and sends an intersystem handover reroute message to SW2, which is the adjacent switch. SW2 replies with an acknowledgement and begins to execute the operations such as authentication, location management from network 1 to network 2. Whereas, the mobile user continues to conduct handover to BS 1 using the standard procedures. When the handover is set up, BS 1 sends a transmitter/receiver start (TXRCVR_start) message.

3.3.2 Handover into a New System

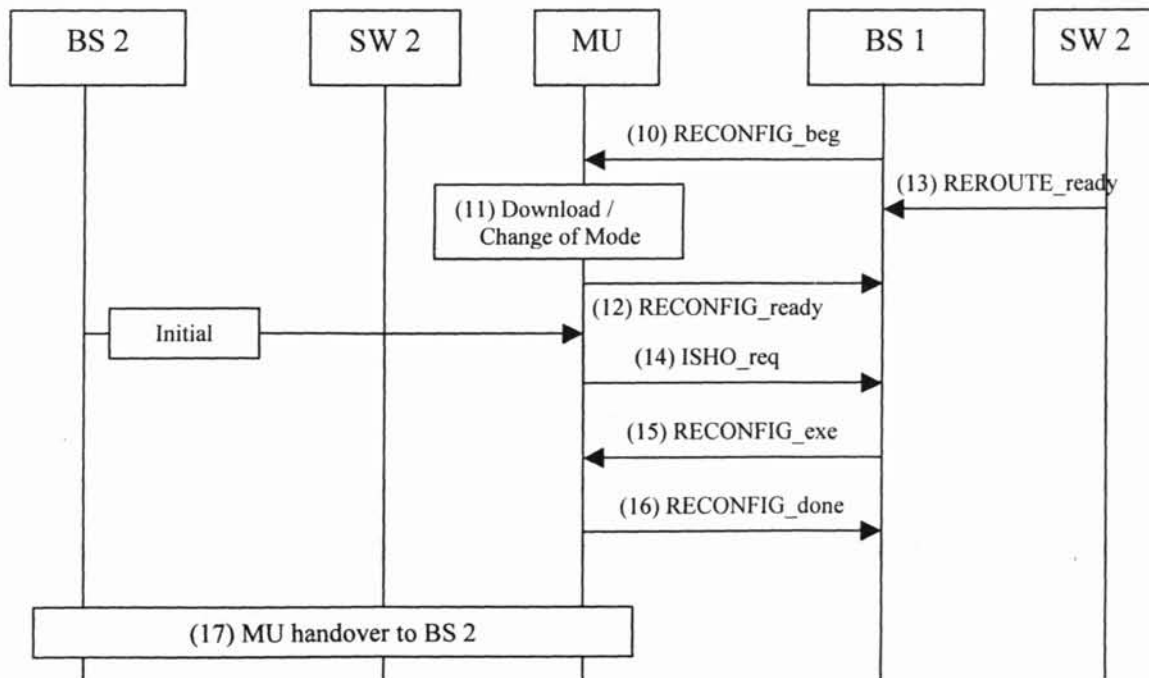


Figure 3-12. Signal flow for Handover into the next system.

where b_i is the size of the control message in bits and R is the bit rate of that link that message is sent.

In step 7, the control message can be sent over N hops from SW1, to a crossover switch between NW1 and NW2, to SW2. If this is the case, then the signaling time is computed by:

$$T_7 = N \times M_7 \quad (3.29)$$

For steps 1, 10, and 14, we need to consider the signaling time for the messages that may be affected by losses over the wireless link. Let n_f be the number of wireless link failures. Then

$$T_i = \sum_{nf=0}^{\infty} T_i(nf) \times \text{prob}\left\{nf \text{ failures and 1 success}\right\} \quad (3.30)$$

Let T_w be the time for waiting in order to decide that the message was lost. The time to send a message when there are n_f failures is calculated:

$$T_i(nf) = M_i + nf \times (T_w + M_i) \quad (3.31)$$

The signaling time, T_i is then represented by:

$$\begin{aligned} T_i &= \sum_{nf=0}^{\infty} [M_i + nf \times (T_w + M_i)] \times \text{prob}\left\{nf \text{ failures and 1 success}\right\} \\ &= M_i + (T_w + M_i) \times \sum_{nf=0}^{\infty} nf \times \text{prob}\left\{nf \text{ failures and 1 success}\right\} \end{aligned} \quad (3.32)$$

3.3.4 Probability of Inter-System Handover Failure

We also need to consider the probability that the inter-system handover fails because of the mobile terminal (MT) leaving the boundary cell before the additional

signaling for the system transformation can be completed. Let T be a random variable that takes on values of the time to the next consecutive handover after the MT's arrival into the boundary cell. Then the probability of the MT leaving the boundary cell before the required time T_{req} is [23]:

$$P = \text{prob}[T < T_{req}] \quad (3.33)$$

We restrict this probability to a certain threshold, P_f . If we assume that T is exponentially distributed then (3.33) will be:

$$\text{prob}[T < T_{req}] < P_f \quad \text{or} \quad 1 - e^{-\lambda T_{req}} < P_f \quad (3.34)$$

Where λ is the arriving rate of MTs into the boundary cell.

$$\lambda_{MT} = \frac{VL}{\pi S} \quad (3.35)$$

Where V is the expected velocity of the MT, l is the length of the perimeter of the boundary cell, and S is the area of the boundary cell [28].

$$\lambda_{MT} = \frac{2V}{\pi l \sin(\pi/3)} \quad (3.36)$$

The minimum boundary cell area can be defined as

$$l > \frac{2VT_{req}}{\pi \log\left(\frac{1}{1-P_f}\right) \sin(\pi/3)}, \quad (3.37)$$

and based on this, the restriction boundary cell area can be obtained from

$$A_{cell} > \frac{6l^2}{2} \sin(\pi/3). \quad (3.38)$$

The system parameters which are applied to analyze the system are listed in Table 5. The MT, BS, and SW processing times, the message size, and the number of hops are input parameters, which are shown in Table 5.

Bit Rate (B) [29], [30]		Propagation Times [26]	
Wire link	155 Mbps	Wireline link	500 μ sec
Wireless Link		Wireless Link	
Low Mobility	2 Mbps	Terrestrial	2 msec
Medium Mobility	384 Kbps	LEO	5.2 ~ 15.2 msec
Vehicular Mobility	144 Kbps	MEO	69 ~ 96 msec
High Mobility	64 Kbps	GEO	239 ~ 270 msec
Satellite Mobility	144 Kbps		
Processing Times (γ)		MT Velocities [31], [27]	
Switch	0.5 msec	Low Mobility	3 km/hr
Base Station	0.5 msec	Medium Mobility	10 ~ 100 km/hr
Mobile User	0.5 msec	High Mobility	300 km/hr
		Nominal Handover Times	
Message Size (b)	50 bytes	PACS	20 msec
Number of Hops	3	DECT	50 msec
Download Time	10 msec	GSM	1 sec
Link Failure probability	0.5		

Table 5. System Parameters.

Table 6 describes the additional signaling time, which is introduced by the inter system handoff protocol and calculated by (3.26). T_s is calculated for the various cell sizes to be supported by IMT-2000, as well as for the Low Earth Orbit (LEO), Medium Earth Orbit (MEO), and Geostationary Orbit (GEO) satellite networks.

	Indoor (Pico)	Pedestrian (micro)	Vehicular (macro)	High Spd (macro)	Satellite Cells		
					LEO	MEO	GEO
V, MU Velocity (Km/hr) [31]	3	3	10 ~ 100	300			
B, Bit rate(bps) [29], [30]	2M	384 k	144 K	64 K	144 K	144 K	144 K
Add'l Signaling Time (sec)	49 m	59 m	80 m	120 m	0.1 ~ 0.2	0.7 ~ 1	2.4 ~ 2.7
Nominal Handover Time (sec) [25]	20 m	50 m	1	1	1	1	1
Total Handover Time (sec)	69 m	109 m	1.1	1.1	1.1 ~ 1.2	1.7 ~ 2	3.6 ~ 4.1

Table 6. Additional Signaling Time Required for Performing Intersystem Handover for IMT-2000.

3.3.5 Boundary cell area

This section describes some observations which are based on the equations of the previous sections. Also, each different network situation is considered [23]. The additional signaling time is a factor that increases the total handover time. From figure 3-12 to figure 3-15, we can see the probability of inter system handover failure is different for each situation. To obtain these probability of ISHO failure graphs (Fig. 3-12~Fig.3-15) we apply the equation of (3.38) and (3.39). It is observed that the smaller the boundary cell area, the less time the mobile terminal needs to execute the format transformation. In other words, the higher the probability of inter system handover failures. There is a higher chance that the mobile terminal may enter the next boundary cell area without the ability to communicate.

The research of [23] indicates that the boundary cell threshold values are reasonable based on the cell size and network type [23]. For example, for the indoor networking case the results shown in figure 3-12, a probability of inter system failure $P_f = 2\%$ the mobile cell area needs to change from a pico cell to a micro cell area of approximately $A_{cell} = 6$ square meters. The minimum boundary cell areas were found in terms of the probability of handover which meets the minimum residing time required for successful handover.

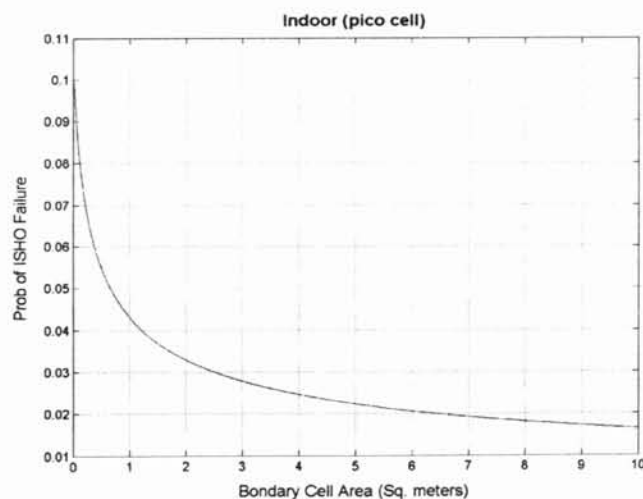


Figure 3-13. Probability of ISHO for Indoor network.

The probability of 2% of ISHO allows a mobile user to roam from a pico cell to a micro cell within a minimum boundary cell area of 6 square meters.

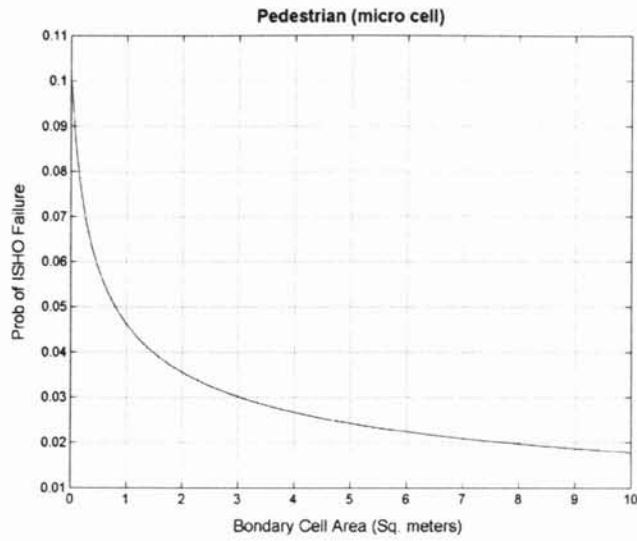


Figure 3-14. Probability of ISHO for Pedestrian network.

The probability of 2% of ISHO allows a mobile user to roam from a micro cell to a macro cell within a minimum boundary cell area of 8 square meters.

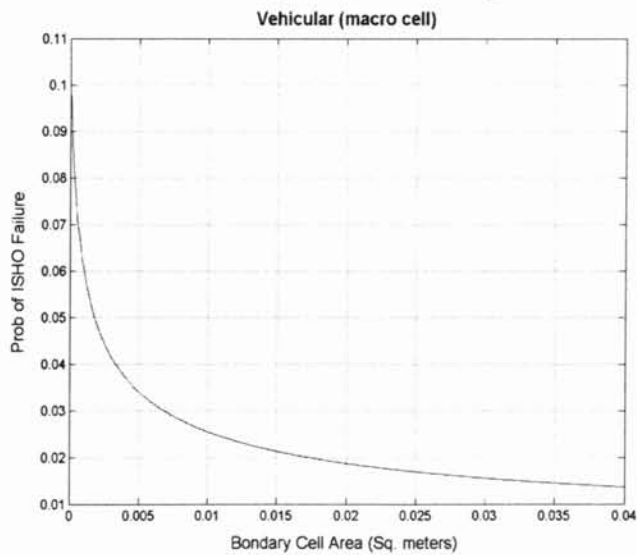


Figure 3-15. Probability of ISHO for vehicular network.

The probability of 2% of ISHO allows a mobile user to roam from a macro cell to another macro cell within a minimum boundary cell area of 0.02 square meters.

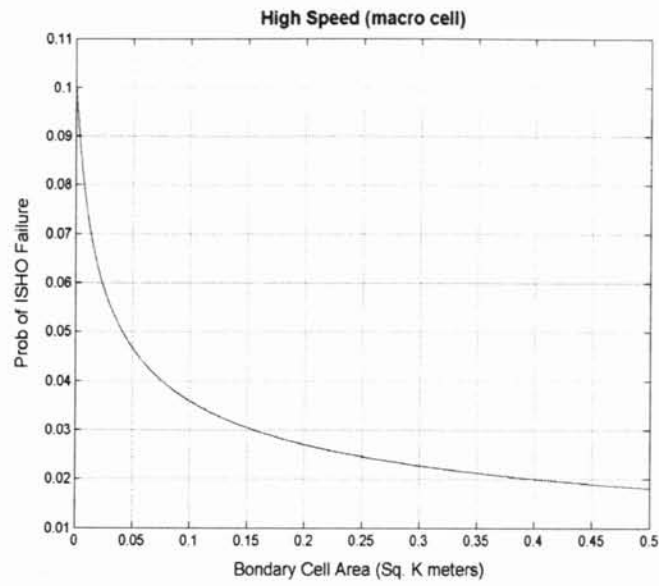


Figure 3-16. Probability of ISHO for high speed network.

The probability of 2% of ISHO allows a mobile user to roam from a macro cell to another macro cell within a minimum boundary cell area of 0.4 square kilo meters

CHAPTER IV

MIMO Systems Based Handover Technologies

As we discuss in chapter 2, there have been many studies devoted to analyze the spectral efficiency of DAA systems. The major concern of the research is placed on the capacity improvement in wireless communication systems. However, the analysis of attainable capacity for DAA systems during handover has not been conducted yet. In this chapter, we analyze the channel capacity during handover for three different system configurations considered in section 2.3.

Section 4.1 provides an introduction of outage capacity analysis and system specifications considered herein.

Capacity outage values for steered array systems, transmitter diversity systems, and DAA systems are analyzed in section 4.2, section 4.3, and section 4.4, respectively.

Comparisons of outage capacity values for those system configurations are also provided in section 4.4.

4.1 Introduction

In this chapter, we analyze the channel capacity supported, when the mobile user migrate from cell A to cell B, as shown in Figure 4-1. If a soft handover scheme is performed, the total capacity obtained at the mobile user is the sum of the capacity values provided by base station A (BS-A) and base station B (BS-B). Throughout this chapter, we analyze the total capacity of three types of system configurations when a mobile user migrates as shown in Figure 4.1, while a soft handover scheme is employed.

As we show in section 3.2, the generalized expression of channel capacity for the dual array antenna is given as:

$$C = B \log_2 \det \left(I + \frac{P_r}{M\sigma^2} H \cdot H^* \right). \quad (4.1)$$

Note that the received signal power depends on the distance between a transmitter and a receiver. Thus, if we denote the channel capacity supported by BS-A as C_A and that

supported by BS-B as C_B , the total capacity supported by both BS-A and BS-B employing soft handover becomes $C_T = C_A + C_B$.

Also, each entries in the channel gain matrix \mathbf{H} in Eq. (4.1) are random, thus, the capacity value is also a random variable, which depends on the location of the receiver and channel states between a transmitter and a receiver. In capacity analysis of wireless communication systems, the outage capacity is of major concern, which represents the capacity value obtained for a given outage. The outage is defined as:

$$Outage = Prob\{C \leq C_{Th}\}, \quad (4.2)$$

where C_{Th} is a threshold capacity value. Specifically, the capacity conditioned value at 10% outage is the threshold value C_{Th} that results in outage probability of 0.1 in Eq. (4.2)

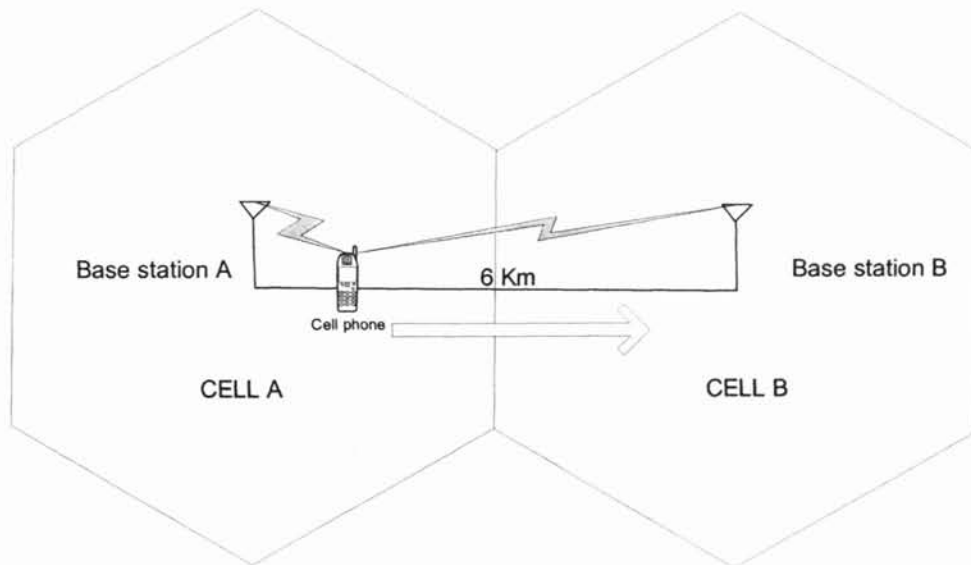


Figure 4-1. Soft handover situation when user is moving from Cell A to Cell B.

As we mentioned in Eq. (2.9), the random behavior of channel gain results in the channel capacity itself random variable. To obtain the statistics of the channel capacity, we generate complex channel gain realization of 10^6 , which includes small scale fading

modeled by rayleigh distribution and large scale shadowing phenomenon modeled by lognormal distribution. From this realization, we compute the channel capacity shown in Eq. (2.10).

The outage of the capacity is given as:

$$Outage = \int_{-\infty}^{C_{Th}} c \cdot dc,$$

where c is statistics of channel capacity, and C_{Th} is a threshold value. In our analysis, we are interested in the capacity value at the target outage probability, which is 10 % in our analysis. Thus, we compute the C_{Th} at the outage probability of 0.1 (10%). The simulation flowchart used to obtain figure 4-4, 4-6, and 4-8 is provided in Appendix A and the actual program is provided in Appendix B. Finally, we compute the channel capacity values at the target outage probability of each system configurations analyzed herein. The capacity values are illustrated in figure 4-4, 4-6, and 4-8.

4.2 Steered directive array system

For steered directive array systems, the closely spaced M antenna elements are mounted on the base station site. The coherently operating array antenna synthesizes the narrow beam pattern such that the signal power is focused to the direction of the targeted mobile user. Since the main-lobe of beam pattern is narrow, the directive array antenna creates less co-channel interference than omni-directional antenna does.

As we show in section 2.3.1, the channel capacity is given as

$$C = B \log_2 \left(1 + \frac{MP_T |h|^2}{\sigma^2} \right) \quad (4.3)$$

where M is the number of antenna elements in steered directive array; h is the complex channel gain.

Capacity values supported by BS-*A* and BS-*B* are shown in Figure 4-2 and actual program is provided in Appendix B (program 1). In the figure, the capacity values at the outage percentage of 10 % are shown, where the dashed lines represent the capacity from base station *A* and the straight lines represent the capacity from base station *B*.

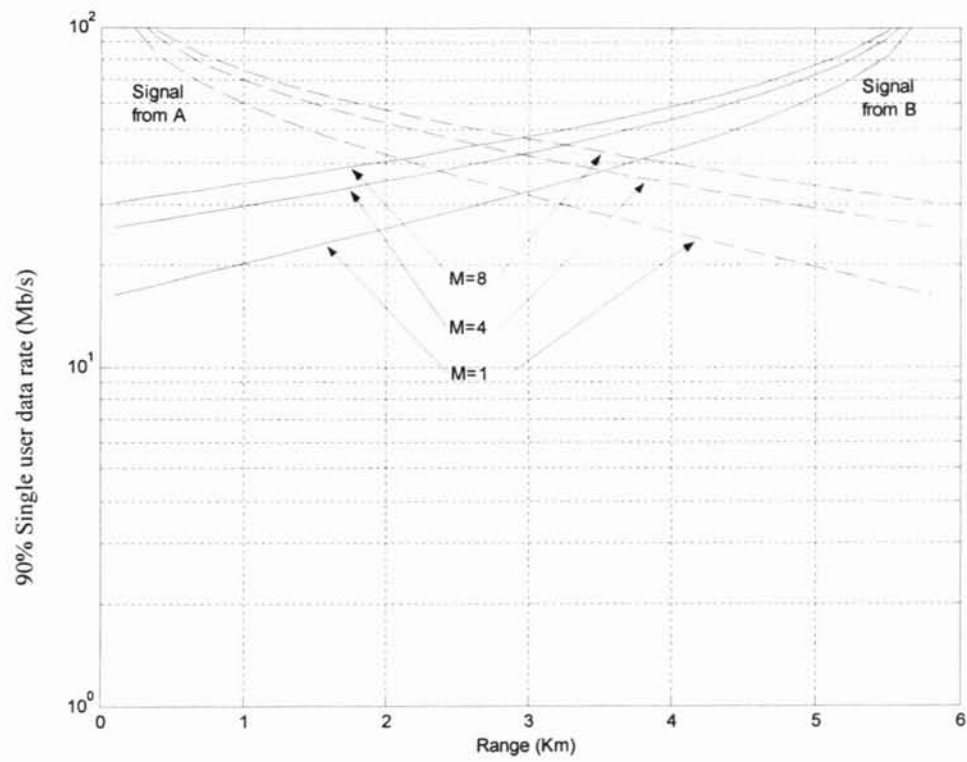


Figure 4-2 Capacity outage vs. distance for the phase steered directive array.

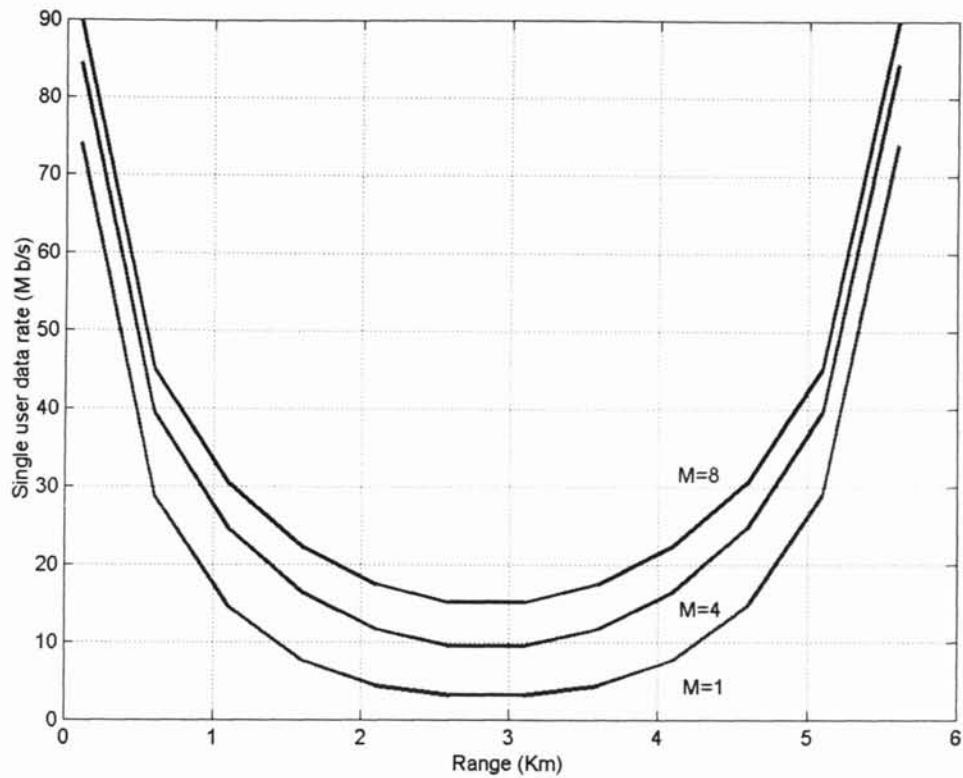


Figure 4-3 Single user data rate vs. distance with the M -steered directive array.

The total capacity values at the outage of 10% are shown in Figure 4-3 and actual program is provided in Appendix B (program 2). The horizontal axis in the figure represents the distance from BS- A to a mobile user. Since the capacity will be poor as the distance is increased, the capacity value at the cell boundary, which is 3 km in our analysis, will be worst performing point. Figure 4.3 shows that capacity is improved as the number of antenna elements in steered directive array are increased. As a example, the capacity values at a distance of 3 km from BS- A are 5 Mb/s for $M=1$, 10 Mb/s for $M=4$ and 16 Mb/s for $M=8$.

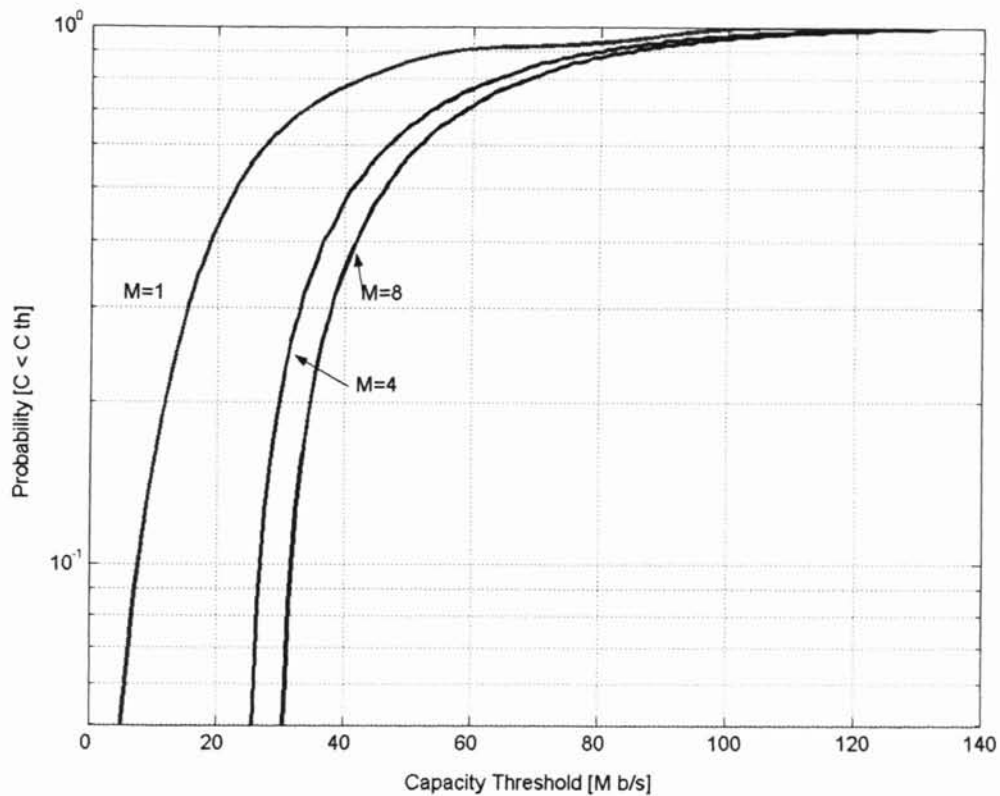


Figure 4-4 Probability of capacity vs. capacity threshold with the steered directive array.

Figure 4-4 shows the outage probability for a capacity threshold value C_{Th} . Thus, the figure shows that the attainable capacity values of an outage probability for all locations of the mobile user shown in Figure 4.1 and actual program is provided in Appendix B (program 3). As an example, when $M = 1$, total capacity obtained at the mobile user at the outage probability of 0.1 (10%) is 10 Mbps. This means that 90 % of locations over the mobile user's migration path, a capacity of 10 Mbps can be provided to the mobile terminal. In a similar fashion, the capacity values at the same outage probability are 25 Mbps and 30 Mbps when $M = 4$ and $M = 8$, respectively. Also, the simulation results show that a 3 times capacity improvement can be obtained when employing an 8 element directive array antenna over single antenna system. Electronic beam steering of directive array antenna system can be achieved by linear phase variation

of each antenna element, provided by the phase shifters across an antenna array. This dynamic variation of phase adjustment enables the array antenna system to change its radiation pattern such that the maximum antenna gain is aligned to the direction of the desired mobile user. Since this phase variation is performed corresponding to carrier frequency, the cost of electronic components for this phase shifter circuit is usually highly expensive. Moreover, the number of phase shifters scales with the number of antenna elements [39]. The same argument for complexity is true to compute the phase shifts for whole antenna elements. Thus, the complexity and the cost of directive steering antenna system is severely limited by the number of antenna elements.

4.3 Transmit diversity system

In the transmitter diversity system the channel capacity is given as:

$$C = B \log_2 \left(1 + \frac{P_T}{M\sigma^2} \sum_{m=1}^M |h_m|^2 \right). \quad (4.4)$$

As we addressed in section 2.3, the transmit diversity system is different from the directive array antenna system in the sense that the antenna element spacing is large enough to ensure uncorrelated channel path gains, and also the total transmission power is limited to P_T , regardless of the number of antenna elements applied.

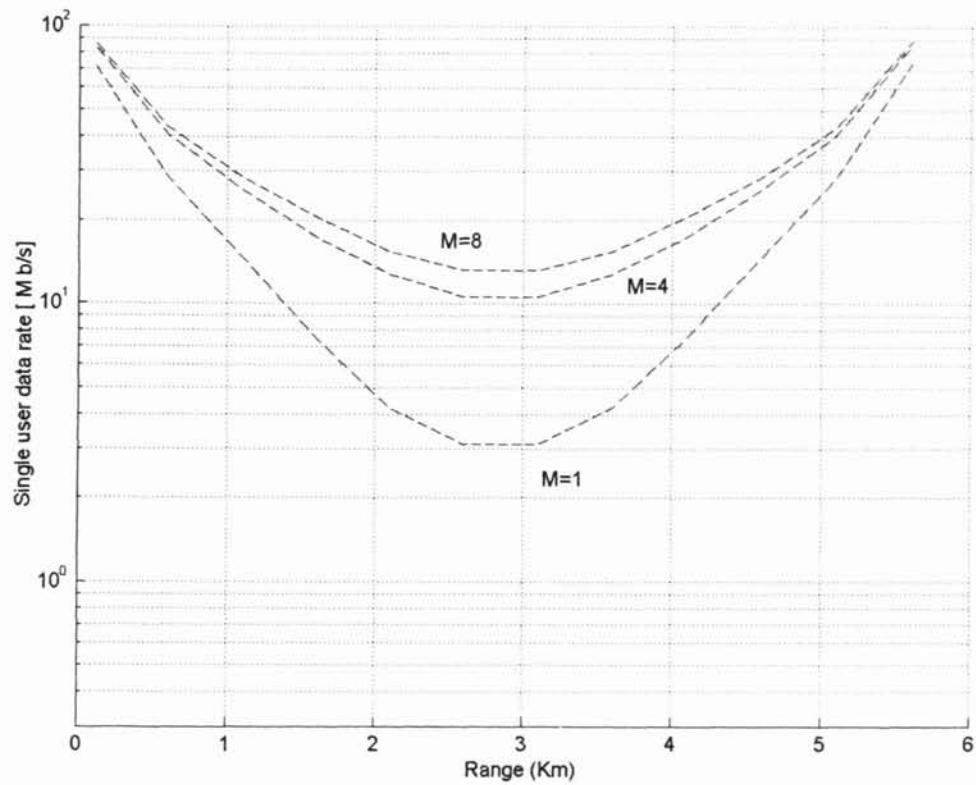


Figure 4-5 Capacity outage vs. distance with the M -antenna transmit diversity.

The capacity supported in 90% of locations is plotted at a different distance in figure 4-5 and actual program is provided in Appendix B (program 4). The simulation results show that the total capacity values are 3 Mb/s for $M=1$, 10 Mb/s for $M=4$ and 15 Mb/s for $M=8$. Compared to the directive array antenna system, the capacity improvement is not noticeable. This is due to the fact that the total transmission power in the transmit diversity system is constrained. In other words, the total transmission power in the directive array antenna system is increased as the number of antenna elements are increased, while that in the transmit diversity system is limited as a constant regardless of the number of antenna elements used.

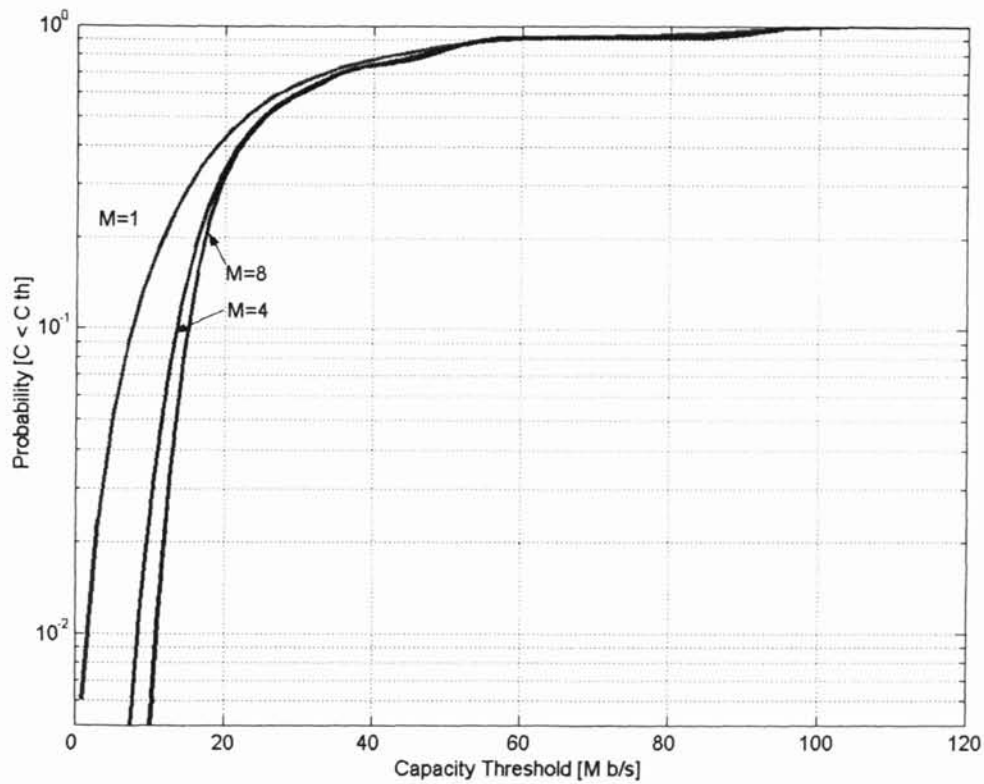


Figure 4-6 Probability of capacity vs. capacity threshold with the transmit diversity.

The attainable capacity values for outage probability are shown in Figure 4.6 and actual program is provided in Appendix B (program 5). It is observed that the total capacity values at the outage of 10% are 10 Mb/s for $M=1$, 16 Mb/s for $M=4$ and 17 Mb/s for $M=8$. Also, it is observed that as M increases from 1 to 8, the capacity increases by about a 1.7 times. A transmit diversity antenna system requires a number of antennas to obtain diversity gain and each antenna requires individual modem for transmitting different information. Since the number of modems equals the number of antennas in the transmit diversity antenna systems, the system cost will increase as the number of antenna grows. This same argument is also true for the DAA systems, which combine the transmit diversity and the receiver diversity and therefore the cost of these systems will be more expensive.

4.4 DAA system

In the DAA systems, independent information is carried over multiple transmit antenna elements simultaneously, while the multiple antenna elements optimally combine the received signal components. The channel capacity of the DAA system is given as:

$$C = B \sum_{i=1}^M \log_2 \left(1 + \frac{P_T}{M\sigma^2} \sum_{j=1}^M |h_{ij}|^2 \right). \quad (4.5)$$

Note that in the following examples, the number of antenna elements (M) at the transmitter is assumed to be the same as that at the receiver.

Figure 4.7 shows the capacity values at the outage probability of 10% for a different number of antenna elements and actual program is provided in Appendix B (program 6). The capacity values at the cell boundary are 60 Mb/s for $M=1$, 150 Mb/s for $M=4$ and 200 Mb/s for $M=8$. Compared to the previous two system configurations, the total capacity obtained in the DAA system during handover is substantially increased as M increases.

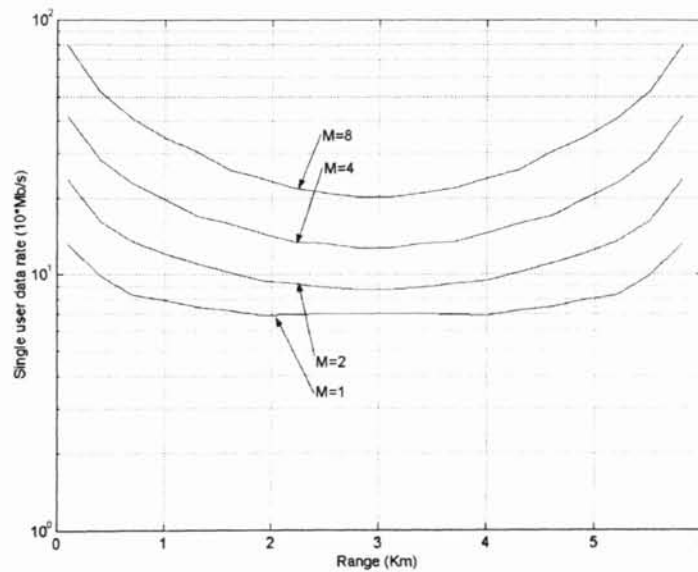


Figure 4-7 Capacity outage vs. distance with the DAA diversity.

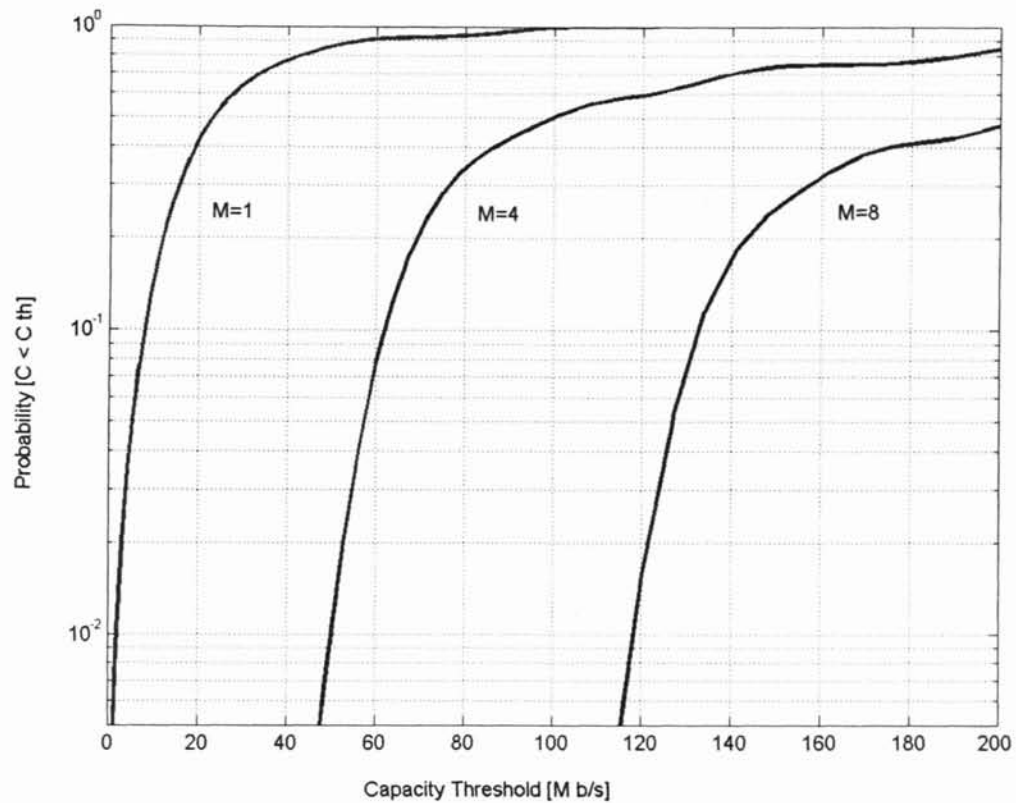


Figure 4-8 Probability of capacity vs. capacity threshold with the DAA system.

The attainable capacity values for outage probability are shown in Figure 4.8 and actual program is provided in Appendix B (program 7). It is observed that the total capacity values at the outage of 10% are 10 Mb/s for $M=1$, 60 Mb/s for $M=4$ and 130 Mb/s for $M=8$. Also, it is observed that as M increases from 1 to 8, the capacity increases by about a 13 times.

As shown in Figure 4-8, the channel capacity of the DAA system grows linearly as the number of antenna increase. Thus, compared to the previous antenna systems, an enormous channel capacity gain can be obtained in the DAA systems by adding additional antennas both at the transmitter and at the receiver sites. Also, notice that the extraordinary growth in data rates is obtained by the combined use of DAA systems.

Capacity Gain at 10 % Outage	$M=1$	$M=4$	$M=8$	Noticeable Characteristics
Directive Array Antenna System	10 Mbps	25 Mbps	30 Mbps	All antenna elements transmit the same signal information. Each antenna transmits P_T [Watts]
Transmit Diversity System	10 Mbps	16 Mbps	17 Mbps	Each antenna transmits different information. All antennas combined together transmit P_T [Watts]
DAA system	10 Mbps	60 Mbps	130 Mbps	M transmit and N receive antennas transmit different information. All antennas combined transmit P_T [Watts]

Table 7. A comparison of the capacity gain for the three topologies.

CHAPTER V

CONCLUSION

In this thesis two fundamental problems relating to handover technology have been investigated.

The prime contribution of this thesis is based on the analysis of the attainable capacity during handover procedures for various MIMO system configurations when soft handover is performed. A comparison of the compared capacity outage probabilities between conventional cellular systems and dual array antenna systems that have gained much attention recently has been conducted.

The directive array antenna synthesis makes the beam pattern narrower as the number of antenna elements increase, such that more power can be launched to the direction of the mobile user, thereby increasing signal power at the receiver. Note that each antenna transmits identical information. The major benefit of the transmit diversity scheme is the physical dimension of a receiver not being a limitation in obtaining diversity gain, since the capacity gain can be obtained by employing additional antenna elements at the transmitter site. Compared to the directive array antenna system, the capacity improvement is not noticeable. This is due to the fact that the total transmission power in the transmit diversity system is constrained. In other words, the total transmission power in the directive array antenna system increases as the number of antenna elements increases, while that in the transmit diversity system is limited as a constant regardless of the number of antenna elements. Therefore, from an interference point of view the transmit diversity system will have an advantage in the Bit Error Rate (BER) performance, although there is no significant capacity gain when compared to the directive antenna array system (small number of M). It is important to note that the drastically growth in attainable outage capacity for the DAA system is provided by the combined use of transmit and receiver simultaneously.

Second a fuzzy logic and LVQ artificial neural network combined algorithm has proposed in support of multivariable optimization in handover decision procedures have been presented. In this proposed model, a Fuzzy logic and LVQ artificial neural network

algorithm was adopted for the handover initiation and decision procedures. In future research we shall implement the fuzzy logic and LVQ network algorithm taking into consideration alternative diversity combining topologies, such as macroscopic and microscopic diversity and error control coding.

CHAPTER VI

References

- [1] V. V. Veeravalli and O. E. Kelly, "A locally handover algorithm for cellular communications," *IEEE Transactions on Vehicular Technology*, vol. 43, no. 3, pp. 603-609, Aug. 1997.
- [2] D. J. Goodman and A. J. Viterbi, *Wireless Personal Communications*. Addison-Wesley, MA: pp. 23-41, Sept. 1997.
- [3] P. Starvroulakis, *Third Generation Mobile Telecommunication Systems: UMTs and IMT-2000*, New York, NY: Springer-Verlag, pp. 520-555, Feb. 2001.
- [4] W. Lee and C. Y. William, *Mobile cellular telecommunications: analog and digital systems*. 2nd Ed., New York, NY: McGraw-Hill, 1995.
- [5] V. K. Grag and J. E. Wilkes, *Principles and Applications of GSM*. Upper Saddle River, NJ: Prentice Hall, pp. 71-109, Sept. 1998.
- [6] L. J. Harte, C. A. Jacobs, and A. D. Smith, *IS-136 TDMA Technology, Economics, and Services*. Norwood, MA: Artech House, pp. 47-109, Oct. 1998.
- [7] Grag, V. Kumar, *IS-95 CDMA and CDMA 2000: Cellular/PCS systems implementation*. Upper Saddle River, NJ: Prentice Hall, 1999.
- [8] K. Buchanan, R. Fudge, T. Phillips, D. Mcfarlane, A. Sasaki, and H. Xia, "IMT-2000: Service Provider's Perspective," *IEEE Personal Communications*. vol. 4, no. 4, pp. 8-13, Aug. 1997.

- [9] R. D. Carsello, F. O'brien, J. A. Tarallo, N. Ziesse, A. Arunachalam, J. M. Costa, R. C. Kirby, A. Maclatchy, F. Watanabe, and H. Xia, "IMT-2000 Standards-Radio Aspects," *IEEE Personal Communication Magazine*, vol. 4, no. 4, pp. 30-40, Aug. 1997.
- [10] R. Pandya, D. Grillo, E. Lycksell, P. Mieybegue, H. Okinaka, and M. Yabusaki, "IMT-2000 Standards: Network Aspects," *IEEE Personal Communication Magazine*, vol. 4, no. 4, pp. 20-29, Aug. 1997.
- [11] ITU-R Rec. M.819-1, "Future public land mobile telecommunication systems (FPLMTS) for developing countries."
- [12] JTC(AIR) 95.06.08-033R3, "Baseline Text for TAG 3(PACS)," Section 6.2, June 8, 1995.
- [13] GSM 05.08 (pr ETS 300 578), *European Digital Cellular Telecommunications system (Phase 2); Radio subsystem Link control*, 3rd ed., May 1995.
- [14] *CDMA System Engineering Training Handbook*-Volume 1. Qualcomm
- [15] R. Vijayan and J. M. Holtzman, "A model for analyzing handover algorithms," *IEEE Transaction on Vehicular Technology*, vol. 42, no. 3, pp.351-356, Aug. 1993.
- [16] G. Edwards and R. Sankar, "Microcellular handover using fuzzy techniques," *ACM Wireless Networks*, vol. 4, pp. 401-409, Sept. 1998.
- [17] G. P. Pollini, "Trends in handover design," *IEEE Communications Magazine*, vol. 34, no. 3, pp. 82-90, Mar. 1996.

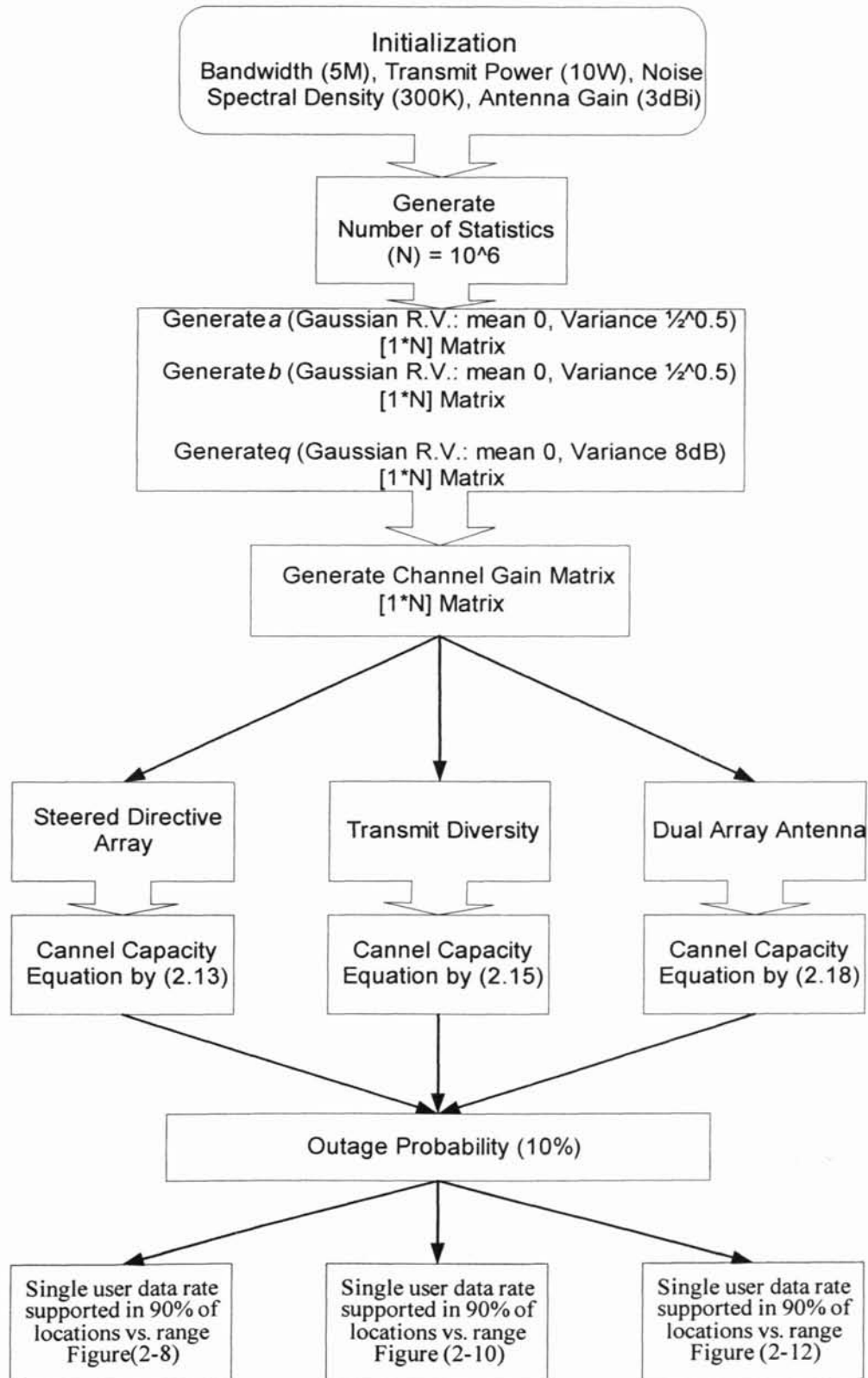
- [18] N. Zhang and J. M. Holtzman, "Analysis of handoff algorithms using both absolute and relative measurements," *IEEE Transactions on Vehicular Technology*, vol. 45, no. 1, pp. 174-179, Feb. 1996.
- [19] T. S. Rappaport, *Wireless Communications: Principles and Practice*. Upper Saddle River, NJ: Prentice-Hall, Dec. 1995.
- [20] P. M. L. Chan, R. E. Sheriff, and Y. F. Hu, "Mobility management incorporating fuzzy logic for a heterogeneous IP environment," *IEEE Communications Magazine*, vol. 39, no. 12, pp. 42-51, Dec. 2001.
- [21] M. T. Hagan, H. B. Demuth, and M. Beale, *Neural networks design*. Boston, MA: PWS Publishing Company, pp. 14/16-14/35, 1996.
- [22] P. Antognetti and V. Milutionovic, *Neural Networks: Concepts, Applications, and Implementations*. Englewood Cliffs, NJ: Prentice-Hall, pp. 124-143, 1991.
- [23] J. McNair, I. F. Akyildiz, and M. D. Bender, "An inter-system handover technique for the IMT-2000 system," *Proceedings of the IEEE INFOCOMM 2000*, vol. 1, pp. 208-216, 2000.
- [24] M. Gudmundson, "Analysis of handover algorithms," *Proceedings of Vehicular technology Conference '91*, St. Louis, MO, pp. 537-542, May 19-22, 1991.
- [25] A. Nospel and Y. B. Lin, "Modeling PCS networks under general call holding time and cell residence time distributions," *IEEE Personal Communications Magazine*, vol. 5, no. 6, pp. 893-906, Dec. 1997.
- [26] N. Efthymiou, Y. F. Hu, and R. Sheriff, "Performance of intersegment handover protocols in an integrated space/terrestrial UMTS environment," *IEEE Transactions on Vehicular Technology*, vol. 47, no. 4, pp. 1179-1199, Nov. 1998.

- [27] Y. B. Lin and I. Chalamtac, "Heterogeneous personal communication services: Integration of PCS systems," *IEEE Communications Magazine*, vol. 34, no. 9, pp. 106-113, Sept. 1996.
- [28] R. Thomas, H. Gilbert, and G. Mazziotto, "Influence of the moving of the mobile stations on the performance of a radio mobile cellular network," *Proceedings of the 3rd Nordic Seminar*, pp. 1-9, Sept. 1988.
- [29] W. Mohr, "European proposal for IMT-2000 part ii: UTRA TDD," *Proceedings of the IMT-2000 Workshop*. Georgia Center for Advanced Telecommunications Technology, Nov. 1998.
- [30] M. Unsoy *et al.*, "IMT-2000: Next generation wireless mobile systems," *Proceedings of the IEEE ICC '98*, June 1998.
- [31] J. G. Markoulidakis, G. L. Lyberopoulos, D. F. Tairkas, and E. D. Sykas, "Mobility modeling in third generation mobile telecommunications systems," *IEEE Personal Communications Magazine*, vol. 4, no. 4, pp. 41-56, Aug. 1997.
- [32] G. J. Foschini and M. J. Gans, "On limits of wireless communications in a fading environment when using multiple antennas," *Wireless Personal Communications*, vol. 6, pp. 311-335, March, 1998.
- [33] C.E. Shannon, "A Mathematical Theory of Communication," *Bell Systems Technical Journal*, vol. 27, pp. 379-423 and pp. 623-656, 1948.
- [34] J. Proakis, *Digital Communications*. New York, NY: McGraw-Hill, 3rd Ed, 1995.

- [35] J. H. Winters, "Signal acquisition and tracking with adaptive arrays in the digital mobile radio system IS-54 with flat fading," *IEEE Transactions on Vehicular Technology*, vol. 42, no. 4, pp. 377-384, Nov. 1993.
- [36] D. C. Cox, "Universal Digital Portable Radio Communications," *Proceedings of IEEE*, vol. 75, no. 4, pp. 436-477, Apr. 1987.
- [37] A. Lozano, F. R. Farrokhi, and R. A. Valenzuela, "Lifting the limits on high speed wireless data access using antenna arrays," *IEEE Communications Magazine*, vol. 39, no. 9, Sept. 2001.
- [38] Y. Lynn, "Optimal and Fuzzy-based handoff algorithms,"
www.stanford.edu/~reinvent/EE359LynnProj.pdf
- [39] B. Elamaran, I. M. Chio, L. Y. Chen, and J. C. Chiao, "Using Reconfigurable PBG Structures for Phase Shifting in a Planar Phased Array," *IEEE International Symposium on Antennas and Propagation and USNC/URSI National Radio Science Meeting*, Salt Lake City, Utah, July 16-21, 2000.

APPENDIX A

The flow chart of capacity for MIMO systems



APPENDIX B

<Program 1> Capacity outage vs. distance for the phase steered directive array.

```
% Name :SDA_1.m
%
% Title: Steered Directive Array Diversity
%
% Synopsis: SDA_1 returns the 10% outage Capacity from BS-A and BS-B for M=[1 4 8]
%
% Date: Nov. 29, 2002
% Author: Jin-Baek Kim
%
% ACSEL & OCLNB Laboratories, School of Electrical & Computer Engineering
% Oklahoma State University, Stillwater, OK 74075
%

% Variable Initializations
n=1e6;           %number of Statistics
BW=5e6;         %Bandwidth is 5 MHz
Pt=10;          %Transmitter power is 10 W
k=1.38e-23;     % Boltzman constant
T=300;          % temperature
G=10^1.5;       % antenna gain 15 dBi
M=[1 4 8];      % number of antenna elements at the Tx
F=10^0.3;       % Noise spectral density
Outage = 90;    % Capacity Outage

Var_LogNorm = 10^.8; % Variance for Lognormal
Var_Rayl = .16;    % Variance for Rayleigh

%Initialization of Matrices
Capo = [];
ff = [];
C_1=[];
C_2=[];

% Generate Gaussian R.V.
a=normrnd(0, sqrt(Var_Ray), M, n); %mean 0 & 1/sqrt(2) variance (Rayleigh)
b=normrnd(0, sqrt(Var_Ray), M, n); %mean 0 & 1/sqrt(2) variance (Rayleigh)

q=normrnd(0,sqrt(Var_LogNorm),M,n); %mean 0 & 8dB variance (lognormal)
phi=a1.^2+b1.^2;
```



```

index=1;
for d=1.0:.5:8.0

    L=-134-35*log10(d)+10*log10(G);

    ohm=10.^(.1*(L+q));
    h_square=phi.*ohm;
    n0=k*T; % Noise spectral density in Watts
    sigma_square=n0*BW*F;

    Capo(1,:)=BW*log2(1+M(1)*Pt*h_square/sigma_square); % Capacity of the system
    Capo(2,:)=BW*log2(1+M(2)*Pt*h_square/sigma_square);
    Capo(3,:)=BW*log2(1+M(3)*Pt*h_square/sigma_square);

    C=Capo;
    C=sort(C, 2); % Sorted Capacity
    Iteration=length(C);

    ff(1,index)=C(1,Iteration*(100-Outage)*1e-2); % 10% Outage Capacity
    ff(2,index)=C(2,Iteration*(100-Outage)*1e-2);
    ff(3,index)=C(3,Iteration*(100-Outage)*1e-2);

    index=index+1

end

C_1=[C_1 ff]

for i=12:-1:1
    Des(1,13-i)=ff(1,i);
    Des(2,13-i)=ff(2,i);
    Des(3,13-i)=ff(3,i);
End

C_2=[C_2 Des]

d=1.0:.5:8.0;
figure(4);

loglog(d, C_1(1,:)/1e6,'r--', d, C_1(2,:)/1e6, 'b--', d, C_1(3,:)/1e6, 'k--');
loglog(d, C_2(1,:)/1e6,'r--', d, C_2(2,:)/1e6, 'b--', d, C_2(3,:)/1e6, 'k--');
axis([1 10 1 1e2]);

```

<Program 2> Single user data rate vs. distance with the steered directive array

```
% Name :SDA_2.m
%
% Title: Steered Directive Array Diversity
%
% Synopsis: SDA_2 returns the sum of 10% outage Capacity for M=[1 4 8]
%
% Date: Nov. 29, 2002
% Author: Jin-Baek Kim
%
% ACSEL & OCLNB Laboratories, School of Electrical & Computer Engineering
% Oklahoma State University, Stillwater, OK 74075
%

% Variable Initializations
n=1e6;           %number of Statistics
BW=5e6;         %Bandwidth is 5 MHz
Pt=10;          %Transmitter power is 10 W
k=1.38e-23;     % Boltzman constant
T=300;          % temperature
G=10^1.5;       % antenna gain 15 dBi
M=[1 4 8];      % number of antenna elements at the Tx
F=10^0.3;       % Noise spectral density
Outage = 90;    % Capacity Outage

Var_LogNorm = 10^.8; % Variance for Lognormal
Var_Rayl = .16;    % Variance for Rayleigh

%Initialization of Matrices
Capo = [];
ff = [];
C_1=[];
C_2=[];

% Generate Gaussian R.V.
a=normrnd(0, sqrt(Var_Ray), M, n); %mean 0 & 1/sqrt(2) variance (Rayleigh)
b=normrnd(0, sqrt(Var_Ray), M, n); %mean 0 & 1/sqrt(2) variance (Rayleigh)

q=normrnd(0,sqrt(Var_LogNorm),M,n); %mean 0 & 8dB variance (lognormal)
phi=a1.^2+b1.^2;

index=1;
for d=1.0:.5:8.0
```

```

L=-134-35*log10(d)+10*log10(G);

ohm=10.^(.1*(L+q));
h_square=phi.*ohm;
n0=k*T; % Noise spectral density in Watts
sigma_square=n0*BW*F;

Capo(1,:)=BW*log2(1+M(1)*Pt*h_square/sigma_square); % Capacity of the system
Capo(2,:)=BW*log2(1+M(2)*Pt*h_square/sigma_square);
Capo(3,:)=BW*log2(1+M(3)*Pt*h_square/sigma_square);

C=Capo;
C=sort(C, 2); % Sorted Capacity
Iteration=length(C);

ff(1,index)=C(1,Iteration*(100-Outage)*1e-2); % 10% Outage Capacity
ff(2,index)=C(2,Iteration*(100-Outage)*1e-2);
ff(3,index)=C(3,Iteration*(100-Outage)*1e-2);

index=index+1

end

C_1=[C_1 ff]

for i=12:-1:1
    Des(1,13-i)=ff(1,i);
    Des(2,13-i)=ff(2,i);
    Des(3,13-i)=ff(3,i);
End

C_2=[C_2 Des]

sum=C_1+C_2;

d=1.0:.5:8.0;
figure(4);
loglog(d, sum(1,:)/1e6,'r-', d, sum(2,:)/1e6, 'b-', d, sum(3,:)/1e6, 'k-');
axis([1 10 1 1e2]);

```

<Program 3> Probability of capacity vs. capacity threshold with the steered directive array

```
% Name :SDA.m
%
% Title: Steered Directive Array Diversity
%
% Synopsis: SDA returns the 10% outage Capacity for M=[1 4 8]
%
% Date: Nov. 29, 2002
% Author: Jin-Baek Kim
%
% ACSEL & OCLNB Laboratories, School of Electrical & Computer Engineering
% Oklahoma State University, Stillwater, OK 74075
%

% Variable Initializations
n=1e6;           %number of Statistics
BW=5e6;         %Bandwidth is 5 MHz
Pt=10;          %Transmitter power is 10 W
k=1.38e-23;     % Boltzman constant
T=300;         % temperature
G=10^1.5;      % antenna gain 15 dBi
M=[1 4 8];     % number of antenna elements at the Tx
F=10^0.3;      % Noise spectral density
Outage = 90;   % Capacity Outage

Var_LogNorm = 10^.8; % Variance for Lognormal
Var_Rayl = .16;    % Variance for Rayleigh

%Initialization of Matrices
Capo = [];
ff = [];

% Generate Gaussian R.V.
a=normrnd(0, sqrt(Var_Ray), M, n); %mean 0 & 1/sqrt(2) variance (Rayleigh)
b=normrnd(0, sqrt(Var_Ray), M, n); %mean 0 & 1/sqrt(2) variance (Rayleigh)

q=normrnd(0,sqrt(Var_LogNorm),M,n); %mean 0 & 8dB variance (lognormal)
phi=a1.^2+b1.^2;

index=1;
for d=1.0:.5:8.0
```

```

L=-134-35*log10(d)+10*log10(G);

ohm=10.^(.1.*(L+q));
h_square=phi.*ohm;
n0=k*T; % Noise spectral density in Watts
sigma_square=n0*BW*F;

Capo(1,:)=BW*log2(1+M(1)*Pt*h_square/sigma_square); % Capacity of the system
Capo(2,:)=BW*log2(1+M(2)*Pt*h_square/sigma_square);
Capo(3,:)=BW*log2(1+M(3)*Pt*h_square/sigma_square);

C=Capo;
C=sort(C, 2); % Sorted Capacity
Iteration=length(C);

ff(1,index)=C(1,Iteration*(100-Outage)*1e-2); % 10% Outage Capacity
ff(2,index)=C(2,Iteration*(100-Outage)*1e-2);
ff(3,index)=C(3,Iteration*(100-Outage)*1e-2);

index=index+1

end

d=1.0:.5:8.0;
figure(4);

loglog(d, ff(1,:)/1e6,'r--', d, ff(2,:)/1e6, 'b--', d, ff(3,:)/1e6, 'k--');
axis([1 10 1 1e2]);

```

<Program 4> Capacity outage vs. distance with the *M*-antenna transmit diversity.

```
% Name :M_Tx_5.m
%
% Title: Transmit Diversity
%
% Synopsis: M_Tx_5 returns the sum of a 10% outage Capacity for M=[1 4 8]
%
% Date: Nov. 29, 2002
% Author: Jin-Baek Kim
%
% ACSEL & OCLNB Laboratories, School of Electrical & Computer Engineering
% Oklahoma State University, Stillwater, OK 74075
%

% Variable Initializations
n=1e6; % number of Statistics
BW=5e6; % Bandwidth is 5 MHz
Pt=10; % Transmitter power is 10 W
k=1.38e-23; % Boltzman constant
F=10^0.3; % 3 dB
T=300; % temperature
n0=k*T; % Noise spectral density in Watts
sigma_square=n0*BW*F;

G=10^1.5; % antenna gain 15 dBi
Outage = 90; % Capacity Outage
Var_LogNorm = 10^.8; % Variance for Lognormal
Var_Ray = .16; % Variance for Rayleigh

%Initialization of Matrices
Capo = [];
Sum_Capo=[];
ff = [];
C_1=[];
C_2=[];

M_Elem=[1 4 8];

for i=1:1:3
    M=M_Elem(i);
    h_square=0;
    index=1;
    for d=0.1:3:6.0
```

```

% Generate Gaussian Random Variables
a=normrnd(0, sqrt(Var_Ray), M, n);    % mean 0 & 1/sqrt(2) variance (Rayleigh)
b=normrnd(0, sqrt(Var_Ray), M, n);    % mean 0 & 1/sqrt(2) variance (Rayleigh)

q = normrnd(0, sqrt(Var_LogNorm), M, n); % mean 0 & 8dB variance (lognormal)

phi=a.^2+b.^2;
L=-134-35*log10(d)+10*log10(G);

ohm=10.^(.1.*(L+q));

h_square=phi.*ohm;
Sub_h = sum(h_square,1);                % Sum of the Channel Gain Matrix

% Capacity of the system

Capo = BW.*log2(1+Pt.*Sub_h./(M*sigma_square)); % Capacity for Tx. Div. Sys.
C=Capo;
C=sort(C, 2);                            % Sorted Capacity
Iteration=length(C);
ff(index)=C(Iteration*(100-Outage)*1e-2); % 10% Outage Capacity
index=index+1

end
C_1=[C_1 ff]

for i=12:-1:1
    Des(1,13-i)=ff(1,i);
    Des(2,13-i)=ff(2,i);
    Des(3,13-i)=ff(3,i);
end
C_2=[C_2 Des]

sum=C_1+C_2;

d=0.1:3:6.0;
figure(2);
hold on;
loglog(d, sum(1,:)/1e6,'r-', d, sum(2,:)/1e6, 'b-', d, sum(3,:)/1e6, 'k-');
axis([0 6 1 1e2]);
end

```

<Program 5> Probability of capacity vs. capacity threshold with the transmit diversity

```
% Name :M_Tx_5.m
%
% Title: Transmit Diversity
%
% Synopsis: M_Tx_5 returns the 10% outage Capacity for M=[1 4 8]
%
% Date: Nov. 29, 2002
% Author: Jin-Baek Kim
%
% ACSEL & OCLNB Laboratories, School of Electrical & Computer Engineering
% Oklahoma State University, Stillwater, OK 74075
%

% Variable Initializations
n=1e6; % number of Statistics
BW=5e6; % Bandwidth is 5 MHz
Pt=10; % Transmitter power is 10 W
k=1.38e-23; % Boltzman constant
F=10^0.3; % 3 dB
T=300; % temperature
n0=k*T; % Noise spectral density in Watts
sigma_square=n0*BW*F;

G=10^1.5; % antenna gain 15 dBi
Outage = 90; % Capacity Outage
Var_LogNorm = 10^.8; % Variance for Lognormal
Var_Ray = .16; % Variance for Rayleigh

%Initialization of Matrices
Capo = [];
Sum_Capo=[];
ff = [];

M_Elem=[1 4 8];

for i=1:1:3
    M=M_Elem(i);
    h_square=0;
    index=1;
    for d=0.1:3:6.0
```



```

% Generate Gaussian Random Variables
a=normrnd(0, sqrt(Var_Ray), M, n);    % mean 0 & 1/sqrt(2) variance (Rayleigh)
b=normrnd(0, sqrt(Var_Ray), M, n);    % mean 0 & 1/sqrt(2) variance (Rayleigh)

q = normrnd(0, sqrt(Var_LogNorm), M, n); % mean 0 & 8dB variance (lognormal)

phi=a.^2+b.^2;
L=-134-35*log10(d)+10*log10(G);

ohm=10.^(.1.*(L+q));

h_square=phi.*ohm;
Sub_h = sum(h_square,1);                % Sum of the Channel Gain Matrix

% Capacity of the system

Capo = BW.*log2(1+Pt.*Sub_h./(M*sigma_square)); % Capacity for Tx. Div. Sys.
C=Capo;
C=sort(C, 2);                            % Sorted Capacity
Iteration=length(C);
ff(index)=C(Iteration*(100-Outage)*1e-2); % 10% Outage Capacity
index=index+1

end

d=0.1:3:6.0;
figure(2);
hold on;
loglog(d, ff./1e6,'b--');

axis([0 6 1 1e2]);
end

```

<Program 6> Capacity outage vs. distance with the DAA diversity system.

```
% Name :MIMO_1.m
%
% Title: MIMO Diversity
%
% Synopsis: MIMO_1 returns the 10% outage Capacity for M=[1 4 8]
%
% Date: Nov. 29, 2002
% Author: Jin-Baek Kim
%
% ACSEL & OCLNB Laboratories, School of Electrical & Computer Engineering
% Oklahoma State University, Stillwater, OK 74075
%

n=1e6;           %number of times
BW=5e6;          % Bandwidth is 5 MHz
Pt=10;           % Transmitter power is 10 W
k=1.38e-23;      % Boltzman constant
F=10^0.3;        % 3 dB
T=300;           % temperature
n0=k*T;          %Noise spectral density in Watts
sigma_square=n0*BW*F;
G=10^1.5;        %antenna gain 15 dBi

Outage = 90;     %Capacity Outage
Var_LogNorm = 10^.8;
Var_Ray = .16;

M=[1 2 4 8];

%Initialization
Sum_Capo=[];
ff = [];

for Elem = 1 : length(M),
    Tmp_M = M(Elem);
    h_square=[];
    index=1;

    Capo = zeros(Tmp_M,n);
```

```

for d=1:10.0
    for capacity_loop = 1 : Tmp_M,
% Generate Gaussian Random Variables
        a=normrnd(0, sqrt(Var_Ray), Tmp_M, n); %mean 0 & 1/sqrt(2) var.(Rayleigh)
        b=normrnd(0, sqrt(Var_Ray), Tmp_M, n); %mean 0 & 1/sqrt(2) var.(Rayleigh)

        q=normrnd(0, sqrt(Var_LogNorm), Tmp_M, n); %mean 0&8dB var. (lognorm)

        phi=a.^2+b.^2;
        ohm = 4*10^(-14)*d^(-3.5)*G*10.^(q./10);
        h_square=phi.*ohm;
        Sub_h = sum(h_square,1);

%Capacity of the system

        Capo(capacity_loop,:) = BW.*log2(1+(Pt/(Tmp_M * sigma_square)).*Sub_h);

        end
        C = sum(Capo, 1);

%Outage
        C=sort(C, 2);
        Iteration=length(C);
        ff(index)=C(Iteration*(100-Outage)*1e-2)
        index=index+1
        Capo = [];
        C = [];

    end

    C_1=[C_1 ff]

    for i=12:-1:1
        Des(1,13-i)=ff(1,i);
        Des(2,13-i)=ff(2,i);
        Des(3,13-i)=ff(3,i);
    end
    C_2=[C_2 Des]

    sum=C_1+C_2;

```

```
d=1:10;
figure(1);
loglog(d, sum(1,:)/1e6, 'r-', d, sum(2,:)/1e6, 'b-', d, sum(3,:)/1e6, 'k-');
axis([1 10 1 1e2]);
hold on;
end
```

<Program 7> Probability of capacity vs. capacity threshold with the DAA diversity.

```
% Name :MIMO.m
%
% Title: MIMO Diversity
%
% Synopsis: MIMO returns the 10% outage Capacity for M=[1 4 8]
%
% Date: Nov. 29, 2002
% Author: Jin-Baek Kim
%
% ACSEL & OCLNB Laboratories, School of Electrical & Computer Engineering
% Oklahoma State University, Stillwater, OK 74075
%
```

```
n=1e6;           %number of times
BW=5e6;          % Bandwidth is 5 MHz
Pt=10;           % Transmitter power is 10 W
k=1.38e-23;      % Boltzman constant
F=10^0.3;        % 3 dB
T=300;           % temperature
n0=k*T;          %Noise spectral density in Watts
sigma_square=n0*BW*F;
G=10^1.5;        %antenna gain 15 dBi
```

```
Outage = 90;     %Capacity Outage
Var_LogNorm = 10^.8;
Var_Ray = .16;
```

```
M=[1 2 4 8];
```

```
%Initialization
Sum_Capo=[];
ff = [];
```

```
for Elem = 1 : length(M),
    Tmp_M = M(Elem);
    h_square=[];
    index=1;

    Capo = zeros(Tmp_M,n);
```

```

for d=1:10.0
    for capacity_loop = 1 : Tmp_M,
% Generate Gaussian Random Variables
        a=normrnd(0, sqrt(Var_Ray), Tmp_M, n); %mean 0 & 1/sqrt(2) var.(Rayleigh)
        b=normrnd(0, sqrt(Var_Ray), Tmp_M, n); %mean 0 & 1/sqrt(2) var.(Rayleigh)

        q=normrnd(0, sqrt(Var_LogNorm), Tmp_M, n); %mean 0&8dB var. (lognorm)

        phi=a.^2+b.^2;
        ohm = 4*10^(-14)*d^(-3.5)*G*10.^(q./10);
        h_square=phi.*ohm;
        Sub_h = sum(h_square,1);

%Capacity of the system

        Capo(capacity_loop,:) = BW.*log2(1+(Pt/(Tmp_M * sigma_square)).*Sub_h);

        end
    C = sum(Capo, 1);

%Outage

    C=sort(C, 2);
    Iteration=length(C);
    ff(index)=C(Iteration*(100-Outage)*1e-2)
    index=index+1
    Capo = [];
    C = [];

    end
    d=1:10;
    figure(1);
    loglog(d, ff./1e6,'r-');
    axis([1 10 1 1e2]);
    hold on;
end

```

VITA 2

Jin-Baek Kim

Candidate for the Degree of

Master of Science

Thesis: IMPROVED HANDOVER PROCESS FOR THE NEXT GENERATION
WIRELESS COMMUNICATION SYSTEMS

Major Field: Electrical Engineering

Biographical:

Personal Data: Born in Chunchon, Korea, On December 4, 1975, the son of
Yoon-Kyoung Kim and Dae-Bock Jang.

Education: Received a Bachelor of Control Engineering from the Kang-Won
National University, Korea in Feb. 2001. Completed the requirements for the
Master of Science degree with a major in Electrical Engineering at the
Oklahoma State University in December 2002.

Experience: Employed as a Research Assistant by the ACSEL and OCLNB
Laboratories, School of Electrical and Computer Engineering, Oklahoma
State University, Jan. 2001 to present.

Employed as a Teaching Assistant for Advanced Wireless Communication
Systems and Telecommunication Systems I at the School of Electrical and
Computer Engineering, Oklahoma State University, Jan. 2001 to Dec. 2001.